Master's Thesis in Computer Science
01 2024

Physical Layer Security for Non-Orthogonal Multiple Access Systems with Short Packet Communications

Hailay Gebremeskel

Faculty of Faculty, Blekinge Institute of Technology, 371 79 Karlskrona, Sweden

This thesis is submitted to the Faculty of Faculty at Blekinge Institute of Technology in partial fulfilment of the requirements for the degree of Master's Thesis in Computer Science. The thesis is equivalent to Weeks weeks of full time studies.

The authors declare that they are the sole authors of this thesis and that they have not used any sources other than those listed in the bibliography and identified as references. They further declare that they have not submitted this thesis at any other institution to obtain a degree.

Contact Information:
Author(s):
Hailay Gebremeskel
E-mail: hage21@student.bth.se

University advisor:
Dr. Thi My Chinh Chu
Department of Computer Science

Faculty of Faculty
Blekinge Institute of Technology
SE–371 79 Karlskrona, Sweden

Internet : www.bth.se
Phone : +46 455 38 50 00
Fax : +46 455 38 50 57

Abstract

This study investigates the physical layer security (PLS) within non-orthogonal multiple access (NOMA) systems in the context of short packet communications (SPC). The primary objective is to obtain a lower block error rate (BLER) and increased secrecy capacity by analyzing different parameters such as the path loss exponent and packet size while fortifying the security of SPC within the NOMA system. The methodology involves mathematical derivations to quantify parameters like signal-to-interference-plus-noise ratio (SINR)/signal-to-noise ratio (SNR) alongside pivotal performance metrics like BLER and Secrecy Capacity. Furthermore, MATLAB will be employed to visualize the impact of varying parameters on BLER and Secrecy Capacity, corroborating the numerical derivations.

Keywords: Physical layer security(PLS), non-orthogonal multiple access (NOMA), short packet communications (SPC), block error rate (BLER),secrecy capacity.

Acknowledgments

I am extremely grateful for the unwavering support and sacrifices made by my brother, Gebrekirstos Gebreselassie. His financial and moral support not only enabled me to complete my master's but also safeguarded my life amidst the atrocities of the genocidal war waged by the Ethiopian and Eritrean governments on the people of Tigray, my community. His contributions extended far beyond tuition fees, His support acted as a lifeline, keeping us together and helping me navigate through the challenges of those troubled times. I extend my heartfelt gratitude not only to Gebrekirstos but also to his partner, Anne, and their family, whose compassion and generosity were pivotal in my journey.

My deepest appreciation goes to my own family. To my wife, whose pregnancy coincided with a period of immense hardship, enduring unimaginable trials while I pursued my studies abroad, including unjust incarceration. Her strength and unwavering encouragement were amazing.

To my brother Dawit, your unwavering support and encouragement for me and my family have been invaluable. To my parents and all my siblings, your diverse forms of support during the harrowing times were crucial to me. Despite everything that occurred, your survival amidst such barbaric atrocities was a beacon of hope in a time of despair.

I am indebted to my advisor, whose guidance and genuine care were instrumental in navigating the challenges of this thesis. Her unwavering support and dedication to her students exemplify the best of mentorship.

I must also extend my gratitude to an anonymous woman whose generosity shone through in my darkest hour. Her financial support, facilitated by Anne, came when my resources were depleted, and my circumstances dire. Additionally, my heartfelt thanks to Gebrecherkos Alemayo, whose unwavering assistance provided much-needed relief during the hard times.

This pursuit of my master's degree serves as a tribute to my beloved nephew, who was more akin to a brother, lost tragically amidst the turmoil. His memory was the guiding force behind my determination to complete this study.

Contents

Chapter 1

Introduction

1.1 Background of Physical Layer Security for Non-Orthogonal Multiple Access Systems with Short Packet Communications

In today's internet world, security of wireless networks is a primary concern. Ensuring the confidentiality and integrity of transmitted information is essential, mainly in cases where sensitive information travels across wireless networks. The idea of securing wireless networks using physical layer properties has emerged as crucial area of study in the recent years.

Physical layer is a backbone of secure communication. It is where all the information gets sent from one place to another. Physical layer security establish secure communication through utilizing physical properties of the wireless channel such as noise, interference, path loss exponent and others without relying solely on encryption methods [3]

While cellular networks have robust security measures, the wireless interface between emerging networks like Internet of Things (IoT) devices and base stations (BS) presents distinct vulnerabilities that demand security measures. Unlike the relatively secure wireless interface between cellphones and BS, the IoT network's wireless interface lacks sufficient security measures [13] for several reasons. IoT devices, characterized by limited computational power, stand as vulnerable targets for various attacks, including eavesdropping. It's within these scenarios that the significance of PLS becomes important.

Non-orthogonal multiple access has emerged as a transformative technique within wireless networks, promising increased spectrum efficiency [5] by enabling multiple user transmissions using shared resources. However, the complexity inherent in simultaneous transmissions within NOMA systems introduces distinct security challenges [1]. Existing security paradigms primarily focus on traditional multiple access techniques, neglecting the specialized vulnerabilities present in NOMA. This gap highlights the need for innovative security protocols explicitly designed to fortify privacy preservation and interference management amid the concurrent access of shared resources within NOMA systems.

Amidst the evolution of wireless networks, the emergence of short packet communications has become pivotal, particularly with its ultra-reliable low-latency communication (URLLC) demands [11]. These data packets serve as critical conduits across numerous applications, especially within IoT networks, where immediate and precise

information exchange is imperative. However, the concise nature of these transmissions amplifies vulnerability to various security threats [11]. Addressing these challenges necessitates tailored security strategies capable of safeguarding transmissions without compromising latency or packet reliability, ensuring the confidentiality and integrity of sensitive information.

While existing literature explores the benefits of NOMA and aspects of PLS in communication systems, there exists a gap in addressing security concerns within NOMA systems handling short packet communications. This thesis aims to bridge this gap by investigating the effect of various parameters on the performance of NOMA systems.

1.2 Scope of the Study

This thesis presents an investigation into increased physical layer security mechanisms within a NOMA system, specifically concerning a base station, two users, and an eavesdropper, all within the context of short packet communications. The methodology encompasses the analysis of signal expressions, SNR/SINR, cumulative distribution functions (CDF), probability density functions (PDF) , block error rates, and secrecy capacity, tailored to the in NOMA setup.

This study employs methodological approach to investigate the performance aspects of NOMA systems within the context of SPC. The primary research objective centers around exploring the performance of NOMA systems, specifically focusing on how various system parameters influence key metrics such as BLER, secrecy capacity, and the implications of SPC on NOMA system performance.

The study concentrates on power domain non-orthogonal multiple access (PD-NOMA) due to its simpler transmit mechanism and lower complexity at the receiver side compared to code domain non-orthogonal multiple access (CD-NOMA) [8]. It examines how power domain multiplexing affects security metrics such as BLER and secrecy capacity within down-link systems, exploring interactions among the base station, users, and eavesdropper.

PD-NOMA allocates different power levels to users based on their channel conditions, with weaker channels receiving higher power allocations from the BS compared to stronger channels. Leveraging superposition coding and successive interference cancellation (SIC) techniques, PD-NOMA enables multiple users to transmit signals simultaneously at the same frequency but with different power levels, and the receiver employs SIC methods to decode these signals in sequence.

The emphasis lies in investigating the NOMA system performance, specifically through deriving equations to calculate SNR, CDF, PDF, BLER, and secrecy capacity and utilize MATLAB to visualize the effect of varying parameters on key performance metrics such as BLER and secrecy capacity.

This study focuses on using the properties of the physical layer pertinent to the specified BS, users, and eavesdropper scenario. It excludes higher layer security protocols or unrelated communication technologies beyond the scope of this defined NOMA setup. Additionally, it excludes extensive hardware implementations beyond the physical layer analysis relevant to the specified base station, users, and eavesdropper scenario.

Anticipated outcomes encompass improved data confidentiality, integrity, and reliability within NOMA setups, guiding the development of more secure and resilient wireless networks.

The thesis begins by establishing the background and significance of physical layer security within NOMA systems, followed by an extensive literature review in Chapter 2. Chapter 3 outlines the methodology employed for analyzing performance within the defined NOMA setup. Subsequent chapters present the performance analysis, result and discussions of these analyses, followed by conclusions and future recommendations.

Chapter 2

Related Work

In [3] the critical aspects of physical layer security within the context of ultra-reliable and low-latency communications have investigate with a focus on ensuring secure and reliable communication with stringent latency requirements. The article delves into fundamental techniques and strategies focused at increasing security in wireless networks, emphasizing the mitigation of eavesdropping threats and ensuring the confidentiality and reliability of transmitted data. They explore various physical layer security mechanisms, considering their applicability in cases demanding ultra-reliability and low-latency communication, which aligns with the general objective of securing wireless network. In the context of my study, this article gives meaningful insights into PLS methodologies applicable to wireless networks. While their focus is on different communication requirements, the fundamental principles and strategies explored in their research contribute to the general understanding of PLS, which can potentially inspire adaptable strategies for increasing security in NOMA systems, mainly when dealing with eavesdropping concerns and ensuring reliable and secure transmissions within latency requirements.

Optimal channel utilization in ultra-reliable short packet relaying communications has studied in [4] with a focus on channel utilization for reliable short packet relaying communications, their exploration aligns with the fundamental aspects of enhancing reliability and efficiency in communication systems, which resonates with the concerns addressed in my study. They primarily delved into the optimization of channel resources for reliability, which indirectly influences security measures due to the inherent relationship between reliability and security in communication systems. While the main focus in [3] is on ensuring secure and reliable communication with stringent latency requirements the focus in [4] is reliability optimization rather than explicitly targeting security improvements. In contrast, my study focuses on utilizing PLS properties to obtain a lower BLER and increased secrecy capacity to increase the performance of the NOMA systems.

In [7], the feasibility and efficacy of half-duplex versus full-duplex relaying has been investigated in wireless networks. Although their study diverges from the context of NOMA systems and physical layer security, their examination of SPC has relevance in understanding the challenges and requirements of secure transmissions. This study primarily delves into the reliability concerns associated with short packet transmissions. Despite the difference in emphasis, their insights into the transmission of short packets in wireless networks can offer valuable insights into the vulnerabilities and reliability issues pertinent to the NOMA system context. The study on PLS for NOMA systems in the context of SPC extends this exploration by concentrating

specifically on the performance challenges within the NOMA systems' setup through analyzing performance metrics such as BLER, and secrecy capacity.

Physical layer security within a full-duplex multi-hop multi-user wireless network employing relay selection has studied in [2]. While their focus was on a different network architecture involving relay nodes, their investigation into PLS aligns with the broader objective of fortifying wireless networks. Their work delves into securing transmissions in a multi-hop setup, considering relay nodes to address security challenges arising from multi-user interactions and relay selections. However, the specific context of their study differs from the scope of my study, which concentrates on the NOMA setups employing SPC. While the focus in [**?**] is on relay selection in multi-hop networks, my study centers on exploring performance metrics tailored for the power domain multiplexing techniques within NOMA systems. Although their work does not directly align with the NOMA setup and SPC methodology addressed in this study, their insights into PLS within multi-hop networks offer valuable perspectives and potential strategies that could inform aspects of security considerations in complex wireless communication systems like NOMA systems.

The critical aspects of secure short packet communications in wireless networks have studied in [6]. The article aims on the importance of physical layer security mechanisms, mainly in the context of short packet communications in 5G and beyond wireless networks. It emphasizes on confidentiality and integrity during the transmission of short packets. They explore various strategies and techniques focused at enhancing security at the physical layer. These approaches likely involve encryption methodologies and channel coding techniques tailored to secure SPC.

In [9], a study has done focusing on short packet down-link transmission utilizing NOMA systems. The study delves into the basic aspects of down-link communication using NOMA, exploring the efficiency of access technique for accommodating short packet transmissions. While their emphasis on [9] resides in enhancing spectral efficiency and system throughput, the emphasis on [6] resides on enhancing security at the physical layer through encryption methodologies and channel coding techniques tailored to secure SPC. Their insights into the down-link transmission setup in NOMA systems align with the fundamental structure of this thesis. Their investigation into short packet transmissions is a groundwork for understanding the dynamics of data transmission in NOMA setups. However, this study diverges by concentrating specifically on the security aspects within the NOMA setup. Where they primarily address transmission efficiency and spectral utilization.

Both [9] and [6] serve as an important reference to understand the fundamental aspects of short packets and could inform the improvement of performance in the context of NOMA systems with a focus on high security against eavesdropping threats and optimizing reliability in SPC. In the context of my study, both articles give meaningful insights into PLS methodologies applicable to wireless networks. While their focus may differ in terms of communication requirements, the fundamental principles and strategies explored in their work contribute to a general understanding of PLS which could inspire adaptable strategies for increasing security in NOMA systems, mainly concerning eavesdropping threats and ensuring reliable and secure transmissions within latency requirements. The study on PLS for NOMA system in the context of SPC extends the discourse by focusing on performance metrics such as BLER, and secrecy capacity pertinent to the NOMA system setup.

The performance of NOMA in the context of SPC has investigated in [12]. The article delves into the performance evaluation of NOMA particularly in the context of SPC. They investigate the suitability of NOMA in scenarios involving short packets, an area of growing importance in modern wireless networks. They conduct a comprehensive analysis, exploring the efficacy of NOMA in accommodating SPC. They likely delve into SNR metrics, BLER, and other relevant parameters crucial for short packet scenarios. While their focus may not have been explicitly on security aspects, their analysis of NOMA's performance in handling short packets could provide valuable insights into potential vulnerabilities or strengths in such scenarios. This article serves as a significant reference, mainly in understanding how NOMA performs in scenarios involving short packets, aligning with the focus of this study on security measures tailored for a NOMA system within a specific setup involving a BS, two users, and an eavesdropper in the context of SPC.

In [10], the optimal power allocation in NOMA visible light communications (VLC) addressing short packets and imperfect channel information has investigated. This work underscores the significance of power allocation strategies in a NOMA system, in the domain of VLC. The consideration of SPC aligns with the focus of my study on analyzing security metrics within a NOMA setup for SPC. Although their investigation revolves around imperfect channel information in VLC, the broader exploration of optimal power allocation shares common ground with the power domain multiplexing analysis within PD-NOMA systems. While [10] concentrates on the optimization of power allocation schemes in a different context [12] concentrates on analyzing short packets. The methodologies employed in [10] could offer insights into power allocation strategies that might influence the security aspects of NOMA systems explored in this study.

Chapter 3

Method

This chapter outlines the methodological approach employed to analyze the performance aspects of NOMA systems within the context of short packet communications. The primary objective of this research is to investigate NOMA system performance, specifically focusing on the impact of system parameters on key metrics like BLER, secrecy capacity, and the implications of SPC on system security and efficiency.

This study concentrates on addressing the following objectives

- Evaluating how different power allocation strategies influence the performance of the NOMA system, with the aim of ascertaining the potential improvement through optimizing the power allocation.
- Analyzing the effects of varying path loss exponents on NOMA system security and reliability.
- Determining the optimal data block size that strikes a balance between latency and system security in NOMA systems with SPC.

This chapter provides the systematic approach adopted to meet these research objectives. It explains the reasoning behind selecting a specific methodological approach, emphasizing its suitability in unraveling the relationships between NOMA system parameters and performance metrics. Moreover, it assesses the reliability and validity of the chosen methodologies, ensuring a robust foundation for subsequent analysis.

3.1 Research Questions

The formulated research questions serve as the cornerstone for exploring the NOMA system performance.
RQ1. How does transmitted power impact the performance of the NOMA system? Can increasing transmitted power allocation improve the NOMA system performance?
RQ2. What effects do different path loss exponents have on NOMA system performance?
RQ3. What is the optimal data block size that effectively balances latency and system security in NOMA systems within SPC?

By examining the relationship between system parameters and performance metrics, this research endeavors to offer valuable insights into optimizing NOMA system

performance and facilitating their practical deployment within wireless communication networks

3.2 Research Method and Design

3.2.1 System Setup

The NOMA system under investigation comprises a BS, two user equipment (UE_1 and UE_2), and an EV). The chosen system utilizes PD-NOMA due to its simplified transmit mechanism and minimal complexity at the receiver side [8]. Additionally, the users operate in half-duplex mode, meaning they only receive data from the BS. Channel coefficients, denoted as h_1, h_2, and h_3, correspond to the channels between UE_1, UE_2, EV, and the BS, as depicted in Figure 3.1.

3.2.2 Mathematical Modeling

The methodology for deriving equations to evaluate SINR/SNR and subsequent performance metrics involves accounting for the relative proximity of the users within the NOMA system architecture. Specifically, it is assumed that UE_1 is in closer proximity to the BS than UE_2, and UE_2 is closer to the BS than the EV.

This consideration of user proximity influences the channel characteristics and subsequently affects the received signal strengths at the BS from each user. The closer proximity of UE_1 to the BS generally results in a stronger received signal compared to UE_2, followed by EV. These relative signal strengths are integral in formulating the equations for SINR/SNR and subsequent performance metrics.

By incorporating this proximity hierarchy into the equations, accounting for channel fading effects and leveraging superposition coding and SIC techniques, the methodology aims to derive comprehensive equations. These equations will facilitate the determination of CDF and PDF of the received signals at the BS.

This approach not only accounts for the inherent differences in the received signal strengths due to varying distances between the entities within the NOMA system but also enriches the derived equations with a realistic representation of the system's physical configuration. The subsequent analysis and visualizations will thus reflect the impact of user proximity on system performance metrics.

3.2.3 Performance Metrics Derivation

The derivation of BLER and secrecy capacity constitutes a fundamental aspect of assessing the performance and security robustness of the NOMA system in the presence of potential eavesdropping attempts.

The BLER calculation involves a meticulous mathematical process accounting for the effects of interference, channel conditions, and power allocation strategies within the NOMA system. By employing superposition coding and successive interference cancellation techniques, the derivation aims to quantify the probability of erroneous decoding of transmitted blocks, thereby providing crucial insights into system reliability under various scenarios.

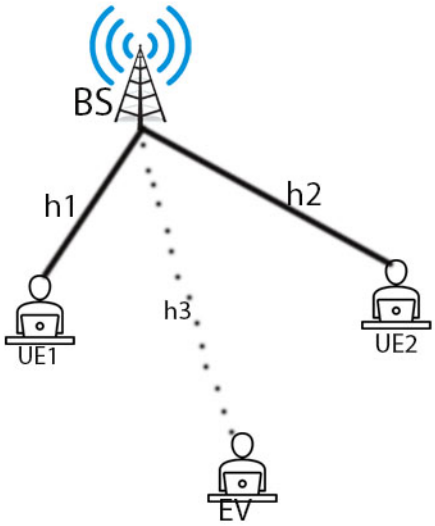

Figure 3.1: System Model

Secrecy capacity, a pivotal metric in evaluating the system's security, requires an intricate mathematical approach. It involves determining the maximum achievable information rate between the legitimate users while minimizing information leakage to the eavesdropper. Through analysis of channel conditions, transmit power, and interference levels, the derivation of secrecy capacity sheds light on the system's ability to maintain confidential communication despite potential adversarial monitoring.

The derived metrics, BLER and secrecy capacity, serve as cornerstone indicators of the NOMA system's performance and resilience against adversarial intrusions. BLER quantifies the reliability of data transmission, whereas secrecy capacity quantifies the system's ability to maintain confidential communication in the presence of an eavesdropper. These metrics offer critical insights into the system's efficacy in real-world scenarios where data integrity and security are paramount concerns.

In essence, the derivation of BLER and secrecy capacity aims at quantifying system performance and security within the NOMA setup. These metrics, play a pivotal role in understanding the system's reliability and security in practical wireless communication scenarios.

3.2.4 Utilization of MATLAB for Visualization

In conjunction with deriving equations, MATLAB serves as a pivotal tool to analyze the impact of varying parameters on BLER and secrecy capacity within the NOMA system setup. Considering the hierarchy of user proximity where UE_1 is closer to the BS than UE_2 and UE_2 is closer to the BS than the EV, MATLAB facilitates the visualization of how alterations in these parameters influence performance metrics.

By systematically adjusting system parameters such as transmit power levels, path loss exponent, and data block sizes, MATLAB generated graphs offer a clear depiction of the consequential variations in BLER and secrecy capacity. These graphical representations provide an intuitive understanding of the system's response to parameter alterations while considering the specific proximity hierarchy among the

system entities.

Assessment of both the derived equations and MATLAB generated graphs is helpful to ensure their relevance within the intended study. Validating the graphical representations against the derived equations ensures the reliability of the analytical method employed.

This utilization of MATLAB aligns with the research objectives focused on evaluating NOMA system performance metrics under varying conditions. The integration of derived equations with visual representations facilitates a clear understanding of performance optimization strategies within the NOMA setup.

3.3 Validity and Reliability

The methodology adopted for this study centered on the derivation of mathematical equations and the subsequent generation of graphs using MATLAB. The equations will be derived to calculate SINR/SNR, CDF, PDF, BLER, secrecy capacity and other parameters within the NOMA system setup. The utilization of MATLAB was solely for visualizing the effects of varying parameters on BLER and secrecy capacity through graphical representations.

The data collection process will involve mathematical derivations based on established principles and theoretical frameworks in wireless communications. This approach ensures a controlled and systematic exploration of NOMA system performance metrics. The analysis relies on mathematical rigor to derive accurate equations and utilize MATLAB generated graphs for visualization purposes.

To ensure reliability, the derived equations will be cross-validated against established theoretical models and sensitivity analyses will be conducted to verify their consistency and accuracy. Moreover, MATLAB-generated graphs will be scrutinized for coherence with the anticipated behavior based on theoretical underpinnings. This process aimed to maintain the validity of the results.

Key strength of the methodology was its structured approach to deriving equations and visualizing performance metrics through MATLAB generated graphs. This approach facilitated a comprehensive analysis of NOMA system behaviors within controlled conditions. However, the study's limitations stem from its reliance on theoretical derivations, potentially limiting the generalizability of findings to real-world scenarios.

In essence, this chapter provides a detailed account of the systematic approach adopted to analyze NOMA system performance metrics. By employing mathematical derivations and MATLAB generated graphs, the study offers valuable insights into the behavior of NOMA systems under various conditions.

However, it is essential to recognize the limitations inherent in the theoretical nature of the study. The findings, while informative within the controlled environment, warrant careful interpretation and further validation in real-world deployments to ascertain their practical applicability.

The critical evaluation underscores the need for future research to bridge the gap between theoretical studies and real-world implementations, thereby enhancing the robustness and applicability of findings in practical wireless communication networks.

Chapter 4

Performance Analysis

4.1 Signal Expression

Assume distance from BS to UE_1 is shorter than distance from BS to UE_2, it follows that the power allocation coefficients $\beta_1 < \beta_2$, where $\beta_1 + \beta_2 = 1$. Let x denotes the superposition signal that is sent out at the BS and can be expressed as

$$x = \sum_{i=1}^{2} \sqrt{\beta_i P} x_i \tag{4.1}$$

Where, x_i represents a transmit signal of UE_i with unit power $|x_i|^2 = 1$, P represents total power sent out at the BS. The signals received at the users can be evaluated as

$$y_j = h_j \sum_{i=1}^{2} \sqrt{\beta_i P} x_i + n_j, for j = 1, 2, 3 \tag{4.2}$$

Where n_j represents an additive white Gaussian noise (AWGN) with zero-mean and variance N_0, j represents UE_1, UE_2 and EV.

UE_2 suffers interference from UE_1, it follows that UE_2 removes UE_1's signal using SIC without the need to decode UE_1's signal while UE_1 needs to decode and cancel UE_2's signal in order to decode its own signal. The signal received at UE_1 can be evaluated as

$$y_1 = h_1 \sqrt{\beta_1 P} x_1 + h_1 \sqrt{\beta_2 P} x_2 + n_1 \tag{4.3}$$

When UE_1 decodes UE_2's Signal at its location, the SINR (γ) can be evaluated as

$$\gamma_{1,2} = \frac{\beta_2 P X_1}{\beta_1 P X_1 + N_0} \tag{4.4}$$

Where $X_i = |h_i|^2$ and N_0 is power spectral density of the noise. UE_1 can extract its own signal by canceling the portion of $h_1 \sqrt{\beta_2 P} x_2$ out of the received signal in equation (4.3). The remaining signal at UE_1 becomes

$$y_1' = h_1 \sqrt{\beta_1 P} x_1 + n_1 \tag{4.5}$$

When, UE_1 decodes its own signal, the SNR (γ) can be evaluated as

$$\gamma_{1,1} = \frac{\beta_1 P X_1}{N_0} \tag{4.6}$$

The final γ at UE_1 can be evaluated as

$$\gamma_1 = \min(\gamma_{1,1}, \gamma_{1,2}) \tag{4.7}$$

The signal received at UE_2 can be evaluated as

$$y_2 = h_2\sqrt{\beta_1 P}x_1 + h_2\sqrt{\beta_2 P}x_2 + n_2 \tag{4.8}$$

UE_2 considers the portion $h_2\sqrt{\beta_1 P}x_1$ as a noise and removes it using SIC. The γ at UE_2 can be evaluated as

$$\gamma_2 = \frac{\beta_2 P X_2}{\beta_1 P X_2 + N_0} \tag{4.9}$$

The signal received at EV can be evaluated as

$$y_3 = h_3\sqrt{\beta_1 P}x_1 + h_3\sqrt{\beta_2 P}x_2 + n_3 \tag{4.10}$$

EV needs to decode both user's signals. EV decodes UE_1's signal as follows. First, EV's signal decodes UE_2 as

$$\gamma_{3,2} = \frac{\beta_2 P X_3}{\beta_1 P X_3 + N_0} \tag{4.11}$$

Second, EV extracts UE_1's signal by canceling the portion of $h_3\sqrt{\beta_2 P}x_2$ out of the received signal in equation (4.10). The remaining signal is given as

$$y_3' = h_3\sqrt{\beta_1 P}x_1 + n_3 \tag{4.12}$$

Finally, EV decodes UE_1's signal as

$$\gamma_{3,1} = \frac{\beta_1 P X_3}{N_0} \tag{4.13}$$

The γ when EV decodes UE_1's signal can be evaluated as

$$\gamma_{E,1} = \min(\gamma_{3,1}, \gamma_{3,2}) \tag{4.14}$$

EV considers the portion $h_3\sqrt{\beta_1 P}x_1$ as a noise and Removes it using SIC. The γ when EV decodes UE_2's signal can be evaluated as

$$\gamma_{E,2} = \frac{\beta_2 P X_3}{\beta_1 P X_3 + N_0} \tag{4.15}$$

4.2 Cumulative Distribution and Probability Density Functions

Let Rayleigh fading affects the channels between the BS and the users and, the channel power gain follows exponential distribution. Assume X_i is exponentially distributed random variable with channel power gain Ω_i.The PDF and CDF of the random variable can be evaluated as

$$f_{X_i}(x) = \frac{1}{\Omega_i}\exp\left(-\frac{x}{\Omega_i}\right) \tag{4.16}$$

$$F_{X_i}(x) = \begin{cases} 1 - \exp\left(-\frac{x}{\Omega_i}\right) & x \geq 0 \\ 0 & x < 0 \end{cases} \tag{4.17}$$

CDF of γ at UE_1 can be evaluated as

$$F_{\gamma_1}(\gamma) = \Pr(\gamma_1 \leq \gamma) \tag{4.18}$$

Substituting γ_1 in equation (4.7) into equation (4.18)

$$F_{\gamma_1}(\gamma) = \Pr(\min(\gamma_{1,1}, \gamma_{1,2}) \leq \gamma) \tag{4.19}$$
$$= 1 - \Pr(\min(\gamma_{1,1}, \gamma_{1,2}) > \gamma) \tag{4.20}$$

Let, $\gamma_{1,1}$ and $\gamma_{1,2}$ are independent random variables. Their probability of occurring together is the product of their individual probabilities

$$F_{\gamma_1}(\gamma) = 1 - \Pr(\gamma_{1,1} > \gamma) \Pr(\gamma_{1,2} > \gamma) \tag{4.21}$$
$$= 1 - (1 - F_{\gamma_{1,1}}(\gamma))(1 - F_{\gamma_{1,2}}(\gamma)) \tag{4.22}$$

$F_{\gamma_{1,1}}(\gamma)$ in equation (4.22) can be evaluated as

$$F_{\gamma_{1,1}}(\gamma) = \Pr(\gamma_{1,1} \leq \gamma) \tag{4.23}$$

Substituting $\gamma_{1,1}$ in equation (4.6) into equation (4.23)

$$F_{\gamma_{1,1}}(\gamma) = \Pr\left(\frac{\beta_1 P X_1}{N_0} \leq \gamma\right) \tag{4.24}$$
$$= F_{X_1}\left(\frac{N_0 \gamma}{\beta_1 P}\right) \tag{4.25}$$

According to equation (4.17), equation (4.25) can be expressed as

$$F_{\gamma_{1,1}}(\gamma) = 1 - \exp\left(-\frac{N_0 \gamma}{\beta_1 \Omega_1 P}\right) \tag{4.26}$$

$F_{\gamma_{1,2}}(\gamma)$ in equation (4.22) can be expressed as

$$F_{\gamma_{1,2}}(\gamma) = \Pr(\gamma_{1,2} \leq \gamma) \tag{4.27}$$

Substituting $\gamma_{1,2}$ in equation (4.4) into equation (4.27)

$$F_{\gamma_{1,2}}(\gamma) = \Pr\left(\frac{\beta_2 P X_1}{\beta_1 P X_1 + N_0} \leq \gamma\right) \tag{4.28}$$
$$= \Pr((\beta_2 - \beta_1 \gamma) P X_1 \leq N_0 \gamma) \tag{4.29}$$

The term $(\beta_2 - \beta_1\gamma)$ in equation (4.29)can be ≥ 0 or < 0.

Case $(\beta_2 - \beta_1\gamma) \geq 0$

$(\beta_2 - \beta_1\gamma) \geq 0 => \frac{\beta_2}{\beta_1} \geq \gamma = \bar{\beta} \geq \gamma$. Where, $\bar{\beta} = \frac{\beta_2}{\beta_1}$

By rearranging equation (4.29), $F_{\gamma_{1,2}}(\gamma)$ can be expressed as

$$F_{\gamma_{1,2}}(\gamma) = \Pr\left(X_1 \leq \frac{N_0 \gamma}{P(\beta_2 - \beta_1 \gamma)}\right) \tag{4.30}$$
$$= F_{X_1}\left(\frac{N_0 \gamma}{P(\beta_2 - \beta_1 \gamma)}\right) \tag{4.31}$$

According to equation (4.17), equation (4.31) can be expressed as

$$F_{\gamma_{1,2}}(\gamma) = 1 - \exp\left(-\frac{N_0\gamma}{P\Omega_1(\beta_2 - \beta_1\gamma)}\right) \tag{4.32}$$

Case $(\beta_2 - \beta_1\gamma). < 0$
$(\beta_2 - \beta_1\gamma) < 0 => \frac{\beta_2}{\beta_1} < \gamma = \bar{\beta} < \gamma$
By rearranging equation (4.29), $F_{\gamma_{1,2}}(\gamma)$ can be expressed as

$$F_{\gamma_{1,2}}(\gamma) = \Pr\left(X_1 > \frac{N_0\gamma}{P(\beta_2 - \beta_1\gamma)}\right) \tag{4.33}$$

$$= 1 \tag{4.34}$$

Combining equations (4.32) and (4.34), $F_{\gamma_{1,2}}(\gamma)$ can be expressed as

$$F_{\gamma_{1,2}}(\gamma) = \begin{cases} 1 & \gamma > \bar{\beta} \\ 1 - \exp\left(-\frac{N_0\gamma}{P\Omega_1(\beta_2 - \beta_1\gamma)}\right) & \gamma \leq \bar{\beta} \end{cases} \tag{4.35}$$

Substituting equations (4.26) and (4.35) into equation (4.22), CDF of γ at UE_1 can be evaluated as

$$F_{\gamma_1}(\gamma) = \begin{cases} 1 & \gamma > \bar{\beta} \\ 1 - \exp\left(-\frac{N_0\gamma}{\beta_1\Omega_1 P}\right)\exp\left(-\frac{N_0\gamma}{P\Omega_1(\beta_2 - \beta_1\gamma)}\right) & \gamma \leq \bar{\beta} \end{cases} \tag{4.36}$$

PDF of γ at UE_1 can be evaluated as

$$f_{\gamma_1}(\gamma) = \frac{\delta(F_{\gamma_1}(\gamma))}{d\gamma} \tag{4.37}$$

$$= \begin{cases} 0 & \gamma > \bar{\beta} \\ \frac{N_0 P\Omega_1\beta_2}{(P\Omega_1(\beta_2 - \beta_1\gamma))^2}\exp\left(-\frac{N_0\gamma}{P\Omega_1(\beta_2 - \beta_1\gamma)}\right)\exp\left(-\frac{N_0\gamma}{\beta_1\Omega_1 P}\right) & \\ \quad + \frac{N_0}{\beta_1\Omega_1 P}\exp\left(-\frac{N_0\gamma}{\beta_1\Omega_1 P}\right)\exp\left(-\frac{N_0\gamma}{P\Omega_1(\beta_2 - \beta_1\gamma)}\right) & \gamma \leq \bar{\beta} \end{cases} \tag{4.38}$$

CDF of γ at UE_2 can be evaluated as as

$$F_{\gamma_2}(\gamma) = \Pr(\gamma_2 \leq \gamma) \tag{4.39}$$

Substituting γ_2 in equation (4.9) into equation (4.39)

$$F_{\gamma_2}(\gamma) = \Pr\left(\frac{\beta_2 P X_2}{\beta_1 P X_2 + N_0} \leq \gamma\right) \tag{4.40}$$

$$= \Pr((\beta_2 - \beta_1\gamma)P X_2 \leq N_0\gamma) \tag{4.41}$$

Case $(\beta_2 - \beta_1\gamma) \geq 0$
Equation (4.41), can be expressed as

$$F_{\gamma_2}(\gamma) = \Pr\left(X_2 \leq \frac{N_0\gamma}{P(\beta_2 - \beta_1\gamma)}\right) \tag{4.42}$$

$$= F_{X_2}(\frac{N_0\gamma}{P(\beta_2 - \beta_1\gamma)}) \tag{4.43}$$

According to equation (4.17), equation (4.43) can be expressed as

$$F_{\gamma_2}(\gamma) = 1 - \exp\left(-\frac{N_0\gamma}{P\Omega_2(\beta_2 - \beta_1\gamma)}\right) \tag{4.44}$$

Case $(\beta_2 - \beta_1\gamma) < 0$
Equation (4.41), can be expressed as

$$F_{\gamma_2}(\gamma) = \Pr\left(X_2 > \frac{N_0\gamma}{P(\beta_2 - \beta_1\gamma)}\right) \tag{4.45}$$

$$= 1 \tag{4.46}$$

Combining equations (4.44) and (4.46)

$$F_{\gamma_2}(\gamma) = \begin{cases} 1 & \gamma > \bar{\beta} \\ 1 - \exp\left(-\frac{N_0\gamma}{P\Omega_2(\beta_2 - \beta_1\gamma)}\right) & \gamma \leq \bar{\beta} \end{cases} \tag{4.47}$$

PDF of γ at UE_2 can be evaluated as

$$f_{\gamma_2}(\gamma) = \frac{\delta(F_{\gamma_2}(\gamma))}{d\gamma} \tag{4.48}$$

$$= \begin{cases} 0 & \gamma > \bar{\beta} \\ \frac{N_0 P\Omega_2\beta_2}{(P\Omega_2(\beta_2 - \beta_1\gamma))^2} \exp\left(-\frac{N_0\gamma}{P\Omega_2(\beta_2 - \beta_1\gamma)}\right) & \gamma \leq \bar{\beta} \end{cases} \tag{4.49}$$

CDF of UE_1's γ at EV can be evaluated as

$$F_{\gamma_{E,1}}(\gamma) = \Pr(\gamma_{E,1} \leq \gamma) \tag{4.50}$$

Substituting $\gamma_{E,1}$ in equation (4.14) into equation (4.50)

$$F_{\gamma_{E,1}}(\gamma) = \Pr(\min(\gamma_{3,1}, \gamma_{3,2}) \leq \gamma) \tag{4.51}$$

$$= 1 - \Pr(\min(\gamma_{3,1}, \gamma_{3,2}) > \gamma) \tag{4.52}$$

Let $\gamma_{3,1}$ and $\gamma_{3,2}$ are independent random variables, their probability of occurring together is the product of their individual probabilities

$$F_{\gamma_{E,1}}(\gamma) = 1 - \Pr(\gamma_{3,1} > \gamma)\Pr(\gamma_{3,2} > \gamma) \tag{4.53}$$

$$= 1 - (1 - F_{\gamma_{3,1}}(\gamma))(1 - F_{\gamma_{3,2}}(\gamma)) \tag{4.54}$$

$F_{\gamma_{3,1}}(\gamma)$ in equation (4.54) can be expressed as

$$F_{\gamma_{3,1}}(\gamma) = \Pr(\gamma_{3,1} \leq \gamma) \tag{4.55}$$

Substituting $\gamma_{3,1}$ in equation (4.13) into equation (4.55)

$$F_{\gamma_{3,1}}(\gamma) = \Pr\left(\frac{\beta_1 P X_3}{N_0} \leq \gamma\right) \tag{4.56}$$

$$= F_{X_3}\left(\frac{N_0\gamma}{\beta_1 P}\right) \tag{4.57}$$

According to equation (4.17), Equation (4.57) can be expressed as

$$F_{\gamma_{3,1}}(\gamma) = 1 - \exp\left(-\frac{N_0\gamma}{\beta_1\Omega_3 P}\right) \tag{4.58}$$

$F_{\gamma_{3,2}}(\gamma)$ in equation (4.54) can be expressed as

$$F_{\gamma_{3,2}}(\gamma) = \Pr(\gamma_{3,2} \leq \gamma) \tag{4.59}$$

Substituting $\gamma_{3,2}$ in equation (4.11) into equation (4.59)

$$F_{\gamma_{3,2}}(\gamma) = \Pr\left(\frac{\beta_2 P X_3}{\beta_1 P X_3 + N_0} \leq \gamma\right) \tag{4.60}$$

$$= \Pr((\beta_2 - \beta_1\gamma)PX_3 \leq N_0\gamma) \tag{4.61}$$

Case $(\beta_2 - \beta_1\gamma) \geq 0$
Equation (4.61) can be expressed as

$$F_{\gamma_{3,2}}(\gamma) = \Pr\left(X_3 \leq \frac{N_0\gamma}{P(\beta_2 - \beta_1\gamma)}\right) \tag{4.62}$$

$$= F_{X_3}(\frac{N_0\gamma}{P(\beta_2 - \beta_1\gamma)}) \tag{4.63}$$

According to equation (4.17), equation (4.63) can be expressed as

$$F_{\gamma_{3,2}}(\gamma) = 1 - \exp\left(-\frac{N_0\gamma}{P\Omega_3(\beta_2 - \beta_1\gamma)}\right) \tag{4.64}$$

Case $(\beta_2 - \beta_1\gamma) < 0$
Equation (4.61) can be expressed as

$$F_{\gamma_{3,2}}(\gamma) = \Pr\left(X_3 > \frac{N_0\gamma}{P(\beta_2 - \beta_1\gamma)}\right) \tag{4.65}$$

$$= 1 \tag{4.66}$$

Combining equations (4.64) and (4.66)

$$F_{\gamma_{3,2}}(\gamma) = \begin{cases} 1 & \gamma > \bar{\beta} \\ 1 - \exp\left(-\frac{N_0\gamma}{P\Omega_3(\beta_2-\beta_1\gamma)}\right) & \gamma \leq \bar{\beta} \end{cases} \tag{4.67}$$

Substituting equations (4.58) and (4.67) into equation (4.54)

$$F_{\gamma_{E,1}}(\gamma) \begin{cases} 1 & \gamma > \bar{\beta} \\ 1 - \exp\left(-\frac{N_0\gamma}{\beta_1\Omega_3 P}\right)\exp\left(-\frac{N_0\gamma}{P\Omega_3(\beta_2-\beta_1\gamma)}\right) & \gamma \leq \bar{\beta} \end{cases} \tag{4.68}$$

PDF of UE_1's γ at EV can be evaluated as

$$f_{\gamma_{E,1}}(\gamma) = \frac{\delta(F_{\gamma_{E,1}}(\gamma))}{d\gamma} \tag{4.69}$$

$$= \begin{cases} 0 & \gamma > \bar{\beta} \\ \frac{N_0 P\Omega_3\beta_2}{(P\Omega_3(\beta_2-\beta_1\gamma))^2}\exp\left(-\frac{N_0\gamma}{P\Omega_3(\beta_2-\beta_1\gamma)}\right)\exp\left(-\frac{N_0\gamma}{\beta_1\Omega_3 P}\right) & \\ \quad + \frac{N_0}{\beta_1\Omega_3 P}\exp\left(-\frac{N_0\gamma}{\beta_1\Omega_3 P}\right)\exp\left(-\frac{N_0\gamma}{P\Omega_3(\beta_2-\beta_1\gamma)}\right) & \gamma \leq \bar{\beta} \end{cases} \tag{4.70}$$

CDF of UE_2's γ at EV can be evaluated as

$$F_{\gamma_{E,2}}(\gamma) = \Pr(\gamma_{E,2} \leq \gamma) \tag{4.71}$$

Substituting $\gamma_{E,2}$ in equation (4.15) into equation (4.71)

$$F_{\gamma_{E,2}}(\gamma) = \Pr\left(\frac{\beta_2 P X_3}{\beta_1 P X_3 + N_0} \leq \gamma\right) \tag{4.72}$$

$$= \Pr((\beta_2 - \beta_1\gamma) P X_3 \leq N_0\gamma) \tag{4.73}$$

Case $(\beta_2 - \beta_1\gamma) \geq 0$
Equation (4.73)can be expressed as

$$F_{\gamma_{3,2}}(\gamma) = \Pr\left(X_3 \leq \frac{N_0\gamma}{P(\beta_2 - \beta_1\gamma)}\right) \tag{4.74}$$

$$= F_{X_3}(\frac{N_0\gamma}{P(\beta_2 - \beta_1\gamma)}) \tag{4.75}$$

According to equation (4.17), equation (4.75) can be expressed as

$$F_{\gamma_{3,2}}(\gamma) = 1 - \exp\left(-\frac{N_0\gamma}{P\Omega_3(\beta_2 - \beta_1\gamma)}\right) \tag{4.76}$$

Case $(\beta_2 - \beta_1\gamma) < 0$
Equation (4.76)can be expressed as

$$F_{\gamma_{3,2}}(\gamma) = \Pr\left(X_3 > \frac{N_0\gamma}{P(\beta_2 - \beta_1\gamma)}\right) \tag{4.77}$$

$$= 1 \tag{4.78}$$

Combining equations (4.76) and (4.78)

$$F_{\gamma_{E,2}}(\gamma) = \begin{cases} 1 & \gamma > \bar{\beta} \\ 1 - \exp\left(-\frac{N_0\gamma}{P\Omega_3(\beta_2 - \beta_1\gamma)}\right) & \gamma \leq \bar{\beta} \end{cases} \tag{4.79}$$

PDF of of UE_2's γ at EV can be evaluated as

$$f_{\gamma_2}(\gamma) = \frac{\delta(F_{\gamma_{E,2}}(\gamma))}{d\gamma} \tag{4.80}$$

$$= \begin{cases} 0 & \gamma > \bar{\beta} \\ \frac{N_0 P\Omega_3\beta_2}{(P\Omega_3(\beta_2 - \beta_1\gamma))^2} \exp\left(-\frac{N_0\gamma}{P\Omega_3(\beta_2 - \beta_1\gamma)}\right) & \gamma \leq \bar{\beta} \end{cases} \tag{4.81}$$

4.3 Short Packets Communications

This thesis examines the performance of the NOMA setup in handling short packets. The primary focus lies in analyzing BLER and secrecy capacity.

4.3.1 Block Error Rate

The BLER that occurs when users decode their signal can be evaluated as

$$\mathcal{E}_i = \int_0^\infty \mathcal{E}_i(\gamma) f_{\gamma_i}(\gamma) d\gamma \tag{4.82}$$

Where, $\mathcal{E}_i$ represents average BLER, $\mathcal{E}_i(\gamma)$ represents instantaneous BLER and $f_{\gamma_i}(\gamma)$ represents PDF. When the channel used is sufficiently large (i.e., m >100), the instantaneous BLER $\mathcal{E}_i(\gamma)$ can tightly be approximated as

$$\mathcal{E}_i(\gamma) \approx \begin{cases} 0 & \gamma \geq \bar{\bar{\gamma}} \\ \frac{1}{2} - \theta_i \sqrt{m}(\gamma - \bar{\theta}_i) & \bar{\gamma} \leq \gamma \leq \bar{\bar{\gamma}} \\ 1 & \gamma \leq \bar{\gamma} \end{cases} \tag{4.83}$$

$$\mathcal{E}_i(\gamma) = \begin{cases} 0 & \gamma \geq \bar{\bar{\gamma}}_i \\ \frac{1}{2} + \theta_i \bar{\theta}_i \sqrt{m} - \theta_i \sqrt{m}\gamma & \bar{\gamma}_i \leq \gamma \leq \bar{\bar{\gamma}}_i \\ 1 & \gamma \leq \bar{\gamma}_i \end{cases} \tag{4.84}$$

Where,

$$r_i = \frac{N_i}{m} \tag{4.85}$$

Where m is the channel use

$$\theta_i = \frac{1}{2\pi\sqrt{2^{2r_i} - 1}} \tag{4.86}$$

$$\bar{\theta}_i = 2^{r_i} - 1 \tag{4.87}$$

$$\bar{\gamma}_i = \bar{\theta}_i - \frac{1}{2\theta_i\sqrt{m}} \tag{4.88}$$

$$\bar{\bar{\gamma}}_i = \bar{\theta}_i + \frac{1}{2\theta_i\sqrt{m}} \tag{4.89}$$

N_i represents the number of bits transmitted from BS to the users
Let, U= $\mathcal{E}_i(\gamma)$ and dV = $f_{\gamma_i}(\gamma)d\gamma$
Equation (4.98) can be rewritten as

$$\mathcal{E}_i = \int_0^\infty U dV \tag{4.90}$$

Where, V=$F_{\gamma_i}(\gamma)$ and U=$\mathcal{E}_i(\gamma)$

$$\int_0^\infty U dV = UV|_0^\infty - \int_0^\infty V dU \tag{4.91}$$

$$dU = \begin{cases} 0 & \gamma \geq \bar{\bar{\gamma}}_i \\ -\theta_i\sqrt{m} & \bar{\gamma}_i \leq \gamma \leq \bar{\bar{\gamma}}_i \\ 0 & \gamma \leq \bar{\gamma}_i \end{cases} \tag{4.92}$$

$UV|_0^\infty$ can be evaluated as

$$UV|_0^\infty = UV|_0^{\bar{\gamma}_i} + UV|_{\bar{\gamma}_i}^{\bar{\bar{\gamma}}_i} + UV|_{\bar{\bar{\gamma}}_i}^{\infty} \tag{4.93}$$

$$\begin{aligned} = & \left(\frac{1}{2} + \theta_i\bar{\theta}_i\sqrt{m} - \theta_i\sqrt{m}\bar{\bar{\gamma}}_i\right) F_{\gamma_i}(\bar{\bar{\gamma}}_i) \\ & + \left(\frac{1}{2} - \theta_i\bar{\theta}_i\sqrt{m} + \theta_i\sqrt{m}\bar{\gamma}_i\right) F_{\gamma_i}(\bar{\gamma}_i) \end{aligned} \tag{4.94}$$

$\int_0^\infty VdU$ can be evaluated as

$$\int_0^\infty VdU = + \int_0^{\bar{\gamma}_i} VdU + \int_{\bar{\gamma}_i}^{\bar{\bar{\gamma}}} VdU + \int_{\bar{\gamma}_i}^{\infty} VdU \tag{4.95}$$

$$= \int_{\bar{\gamma}_i}^{\bar{\bar{\gamma}}} VdU \tag{4.96}$$

Substituting V, and dU for the interval $\bar{\gamma}_i \leq \gamma \leq \bar{\bar{\gamma}}_i$ in equation (4.92) into equation (4.96)

$$\int_0^\infty VdU = \theta_i\sqrt{m} \int_{\bar{\gamma}_i}^{\bar{\bar{\gamma}}_i} F_{\gamma_i}(\gamma)d\gamma \tag{4.97}$$

Substituting equations (4.94) and (4.97) into equation (4.91)

$$\int_0^\infty UdV = \bar{\mathcal{E}}_i - \theta\sqrt{m} \int_{\bar{\gamma}}^{\bar{\bar{\gamma}}} F_{\gamma_i}(\gamma)d\gamma \tag{4.98}$$

Where,

$$\begin{aligned} \bar{\mathcal{E}}_i = & \left(\frac{1}{2} + \theta_i\bar{\theta}_i\sqrt{m} - \theta_i\sqrt{m}\bar{\bar{\gamma}}_i\right) F_{\gamma_i}(\bar{\bar{\gamma}}_i) \\ & + \left(\frac{1}{2} - \theta_i\bar{\theta}_i\sqrt{m} + \theta_i\sqrt{m}\bar{\gamma}_i\right) F_{\gamma_i}(\bar{\gamma}_i) \end{aligned}$$

Substituting equation (4.98) into equation (4.90)

$$\mathcal{E}_i = \bar{\mathcal{E}}_i - \theta_i\sqrt{m} \int_{\bar{\gamma}_i}^{\bar{\bar{\gamma}}_i} F_{\gamma_i}(\gamma)d\gamma \tag{4.99}$$

The BLER when UE_1 decodes its own signal can be evaluated as

$$\mathcal{E}_1 = \bar{\mathcal{E}}_1 + \theta_1\sqrt{m} \int_{\bar{\gamma}_1}^{\bar{\bar{\gamma}}_1} F_{\gamma_1}(\gamma)d\gamma \tag{4.100}$$

$F_{\gamma_1}(\gamma)$ depends on $\bar{\beta}$. Based on $\bar{\beta}$, $\mathcal{E}_1$ can be evaluated in three cases.

Case $\bar{\beta} < \bar{\gamma}_1$

$$\mathcal{E}_1 = \bar{\mathcal{E}}_1 + \theta_1\sqrt{m} \int_{\bar{\gamma}_1}^{\bar{\bar{\gamma}}_1} F_{\gamma_1}(\gamma)d\gamma \tag{4.101}$$

Substituting $F_{\gamma_1}(\gamma)$ in equation (4.36) for $\gamma > \bar{\beta}$ into equation (4.101)

$$\mathcal{E}_1 = \bar{\mathcal{E}}_1 + \theta_1\sqrt{m}(\bar{\bar{\gamma}}_1 - \bar{\gamma}_1) \tag{4.102}$$

Substituting $\bar{\bar{\gamma}}_1$ and $\bar{\gamma}_1$ in equation (4.89) and (4.88) into equation (4.102)

$$\mathcal{E}_1 = \bar{\mathcal{E}}_1 + \theta_1\sqrt{m}(\bar{\theta}_1 + \frac{1}{2\theta_1\sqrt{m}} - \bar{\theta}_1 + \frac{1}{2\theta_1\sqrt{m}}) \tag{4.103}$$

$$= \bar{\mathcal{E}}_1 + 1 \tag{4.104}$$

Case $\bar{\gamma}_1 \leq \bar{\beta} < \bar{\bar{\gamma}}_1$

$$\mathcal{E}_1 = \bar{\mathcal{E}}_1 + \theta_1\sqrt{m}\left(\int_{\bar{\gamma}_1}^{\bar{\beta}} F_{\gamma_1}(\gamma)d\gamma + \int_{\bar{\beta}}^{\bar{\bar{\gamma}}_1} F_{\gamma_1}(\gamma)d\gamma\right) \tag{4.105}$$

Substituting $F_{\gamma_1}(\gamma)$ in equation (4.36) into equation (4.105)

$$\begin{aligned}\mathcal{E}_1 &= \bar{\mathcal{E}}_1 + \theta_1\sqrt{m}\int_{\bar{\gamma}_1}^{\bar{\beta}}\left(1 - \exp\left(\frac{-N_0\gamma}{\beta_1\Omega_1 P}\right)\exp\left(\frac{-N_0\gamma}{P\Omega_1(\beta_2 - \beta_1\gamma)}\right)\right)d\gamma \\ &\quad + \theta_1\sqrt{m}\int_{\bar{\beta}}^{\bar{\bar{\gamma}}_1} 1\, d\gamma\end{aligned} \tag{4.106}$$

$$\begin{aligned}&= \bar{\mathcal{E}}_1 + \theta_1\sqrt{m}(\bar{\bar{\gamma}}_1 - \bar{\gamma}_1) \\ &\quad - \theta_1\sqrt{m}\int_{\bar{\gamma}_1}^{\bar{\beta}} \exp\left(-\frac{(\beta_2\Omega_1 N_0\gamma - \beta_1\Omega_2 N_0\gamma^2) + \beta_1\Omega_1 N_0\gamma}{\beta_1\Omega_1 P\Omega_1(\beta_2 - \beta_1\gamma)}\right)d\gamma\end{aligned} \tag{4.107}$$

Substituting $\bar{\bar{\gamma}}_1$ in equation (4.89) and $\bar{\gamma}_1$ in equation (4.88) into equation (4.107)

$$\mathcal{E}_1 = 1 + \bar{\mathcal{E}}_1 - \theta_1\sqrt{m}\int_{\bar{\gamma}_1}^{\bar{\beta}} \exp\left(\frac{-N_0\gamma}{\beta_1\Omega_1 P} - \frac{N_0\gamma}{P\Omega_1(\beta_2 - \beta_1\gamma)}\right)d\gamma \tag{4.108}$$

We have, $\int_a^b \exp(-A(x))dx = \frac{1}{\frac{\delta(-A(x))}{dx}}\exp(-A(x))|_a^b$

$$\int_{\bar{\gamma}_1}^{\bar{\beta}} A d\gamma = \frac{1}{\frac{\delta\left(\frac{-N_0\gamma}{\beta_1\Omega_1 P} - \frac{N_0\gamma}{P\Omega_1(\beta_2-\beta_1\gamma)}\right)}{d\gamma}}\exp(\frac{-N_0\gamma}{\beta_1\Omega_1 P} - \frac{N_0\gamma}{P\Omega_1(\beta_2 - \beta_1\gamma)})|_{\bar{\gamma}_1}^{\bar{\beta}} \tag{4.109}$$

$$= \frac{1}{-\frac{N_0}{\beta_1\Omega_1 P} - \frac{N_0\Omega_1 P\beta_2}{(\Omega_1 P(\beta_2-\beta_1\gamma))^2}}\exp\left(\frac{-N_0\gamma}{\beta_1\Omega_1 P} - \frac{N_0\gamma}{P\Omega_1(\beta_2 - \beta_1\gamma)}\right)|_{\bar{\gamma}_1}^{\bar{\beta}} \tag{4.110}$$

Where, A $= \exp\left(\frac{-N_0\gamma}{\beta_1\Omega_1 P} - \frac{N_0\gamma}{P\Omega_1(\beta_2-\beta_1\gamma)}\right)$
Substituting equation (4.110) into equation (4.108)

$$\begin{aligned}\mathcal{E}_1 = 1 + \bar{\mathcal{E}}_1 &- \frac{\theta_1\sqrt{m}}{\frac{-N_0}{\beta_1\Omega_1 P} - \frac{N_0\Omega_1 P\beta_2}{(\Omega_1 P(\beta_2-\beta_1\bar{\beta}))^2}}\exp\left(\frac{-N_0\bar{\beta}}{\beta_1\Omega_1 P} - \frac{N_0\bar{\beta}}{P\Omega_1(\beta_2 - \beta_1\bar{\beta})}\right) \\ &+ \frac{\theta_1\sqrt{m}}{\frac{-N_0}{\beta_1\Omega_1 P} - \frac{N_0\Omega_1 P\beta_2}{(\Omega_1 P(\beta_2-\beta_1\bar{\gamma}_1))^2}}\exp\left(\frac{-N_0\bar{\gamma}_1}{\beta_1\Omega_1 P} - \frac{N_0\bar{\gamma}_1}{P\Omega_1(\beta_2 - \beta_1\bar{\gamma}_1)}\right)\end{aligned} \tag{4.111}$$

Case $\bar{\beta} \geq \bar{\bar{\gamma}}_1$

$$\mathcal{E}_1 = \bar{\mathcal{E}}_1 + \theta_1\sqrt{m}\int_{\bar{\gamma}_1}^{\bar{\bar{\gamma}}_1} F_{\gamma_1}(\gamma)d\gamma \tag{4.112}$$

Substituting $F_{\gamma_1}(\gamma)$ for $\gamma \leq \bar{\beta}$ in equation (4.36) into equation (4.112)

$$\mathcal{E}_1 = \bar{\mathcal{E}}_1 + \theta_1\sqrt{m}\left(\int_{\bar{\gamma}_1}^{\bar{\bar{\gamma}}_1} 1 - \exp\left(\frac{-N_0\gamma}{\beta_1\Omega_1 P}\right)\exp\left(\frac{-N_0\gamma}{P\Omega_1(\beta_2-\beta_1\gamma)}\right)d\gamma\right) \tag{4.113}$$

$$= \bar{\mathcal{E}}_1 + 1 - \theta_1\sqrt{m}\int_{\bar{\gamma}_1}^{\bar{\bar{\gamma}}_1}\exp\left(-\frac{N_0\gamma}{\beta_1\Omega_1 P} - \frac{N_0\gamma}{P\Omega_1(\beta_2-\beta_1\gamma)}\right)d\gamma \tag{4.114}$$

By Replacing the interval $|_{\bar{\gamma}_1}^{\bar{\beta}}$ by $|_{\bar{\gamma}_1}^{\bar{\bar{\gamma}}_1}$ in equation (4.110) equation (4.114) can be expressed as

$$\begin{aligned}\mathcal{E}_1 = \bar{\mathcal{E}}_1 + 1 &- \frac{\theta_1\sqrt{m}}{\frac{-N_0}{\Omega_1 P\beta_1} - \frac{N_0\Omega_1 P\beta_2}{(\Omega_1 P(\beta_2-\beta_1\bar{\bar{\gamma}}_1))^2}}\exp\left(\frac{-N_0\bar{\bar{\gamma}}_1}{\beta_1\Omega_1 P} - \frac{N_0\bar{\bar{\gamma}}_1}{P\Omega_1(\beta_2-\beta_1\bar{\bar{\gamma}}_1)}\right)\\ &+\frac{\theta_1\sqrt{m}}{\frac{-N_0}{\beta_1\Omega_1 P} - \frac{N_0\Omega_1 P\beta_2}{(\Omega_1 P(\beta_2-\beta_1\bar{\gamma}_1))^2}}\exp\left(\frac{-N_0\bar{\gamma}_1}{\beta_1\Omega_1 P} - \frac{N_0\bar{\gamma}_1}{P\Omega_1(\beta_2-\beta_1\bar{\gamma}_1)}\right)\end{aligned} \tag{4.115}$$

Combining equations (4.104), (4.111) and (4.115), $\mathcal{E}_1$ can be expressed as

$$\mathcal{E}_1 = \begin{cases} \bar{\mathcal{E}}_1 + 1 & \bar{\beta} < \bar{\gamma}_1 \\ \bar{\mathcal{E}}_1 + 1 - \frac{\theta_1\sqrt{m}}{\frac{-N_0}{\beta_1\Omega_1 P} - \frac{N_0\Omega_1 P\beta_2}{(\Omega_1 P(\beta_2-\beta_1\bar{\beta}))^2}}\exp\left(\frac{-N_0\bar{\beta}}{\beta_1\Omega_1 P} - \frac{N_0\bar{\beta}}{P\Omega_1(\beta_2-\beta_1\bar{\beta})}\right) & \\ \quad + \frac{\theta_1\sqrt{m}}{\frac{-N_0}{\beta_1\Omega_1 P} - \frac{N_0\Omega_1 P\beta_2}{(\Omega_1 P(\beta_2-\beta_1\bar{\gamma}_1))^2}}\exp\left(\frac{-N_0\bar{\gamma}_1}{\beta_1\Omega_1 P} - \frac{N_0\bar{\gamma}_1}{P\Omega_1(\beta_2-\beta_1\bar{\gamma}_1)}\right) & \bar{\gamma}_1 \leq \bar{\beta} < \bar{\bar{\gamma}}_1 \\ \bar{\mathcal{E}}_1 + 1 - \frac{\theta_1\sqrt{m}}{\frac{-N_0}{\beta_1\Omega_1 P} - \frac{N_0\Omega_1 P\beta_2}{(\Omega_1 P(\beta_2-\beta_1\bar{\bar{\gamma}}_1))^2}}\exp\left(\frac{-N_0\bar{\bar{\gamma}}_1}{\beta_1\Omega_1 P} - \frac{N_0\bar{\bar{\gamma}}_1}{P\Omega_1(\beta_2-\beta_1\bar{\bar{\gamma}}_1)}\right) & \\ \quad - \frac{\theta_1\sqrt{m}}{\frac{-N_0}{\beta_1\Omega_1 P} - \frac{N_0\Omega_1 P\beta_2}{(\Omega_1 P(\beta_2-\beta_1\bar{\gamma}_1))^2}}\exp\left(\frac{-N_0\bar{\gamma}_1}{\beta_1\Omega_1 P} - \frac{N_0\bar{\gamma}_1}{P\Omega_1(\beta_2-\beta_1\bar{\gamma}_1)}\right) & \bar{\beta} \geq \bar{\bar{\gamma}}_1 \end{cases} \tag{4.116}$$

$\Omega_1 = d_1^{-n}$. Where d_1 is distance from BS to UE_1 and n is Path loss exponent.

The BLER when UE_2 decodes its own signal can be evaluated as

$$\mathcal{E}_2 = \bar{\mathcal{E}}_2 + \theta_2\sqrt{m}\int_{\bar{\gamma}_2}^{\bar{\bar{\gamma}}_2} F_{\gamma_2}(\gamma)d\gamma \tag{4.117}$$

Based on $\bar{\beta}$, $\mathcal{E}_2$ can be evaluated in three cases.

Case $\bar{\beta} < \bar{\gamma}_2$

$$\mathcal{E}_2 = \bar{\mathcal{E}}_2 + \theta_2\sqrt{m}\int_{\bar{\gamma}_2}^{\bar{\bar{\gamma}}_2} F_{\gamma_2}(\gamma)d\gamma \tag{4.118}$$

Substituting $F_{\gamma_2}(\gamma)$ in equation (4.47) for $\gamma > \bar{\beta}$ into equation (4.118)

$$\mathcal{E}_2 = \bar{\mathcal{E}}_2 + \theta_2\sqrt{m}\int_{\bar{\gamma}_2}^{\bar{\bar{\gamma}}_2} 1 d\gamma \tag{4.119}$$

$$= \bar{\mathcal{E}}_2 + \theta_2\sqrt{m}(\bar{\bar{\gamma}}_2 - \bar{\gamma}_2) \tag{4.120}$$

Substituting $\bar{\bar{\gamma}}_2$ and $\bar{\gamma}_2$ in equation (4.89) and (4.88) into equation (4.120)

$$\mathcal{E}_2 = \bar{\mathcal{E}}_2 + \theta_2\sqrt{m}(\bar{\theta}_2 + \frac{1}{2\theta_2\sqrt{m}} - \bar{\theta}_2 + \frac{1}{2\theta_2\sqrt{m}}) \tag{4.121}$$

$$= \bar{\mathcal{E}}_2 + 1 \tag{4.122}$$

Case $\bar{\gamma}_2 \leq \bar{\beta} < \bar{\bar{\gamma}}_2$

$$\mathcal{E}_2 = \bar{\mathcal{E}}_2 + \theta_2\sqrt{m}\left(\int_{\bar{\gamma}_2}^{\bar{\beta}} F_{\gamma_2}(\gamma)d\gamma + \int_{\bar{\beta}}^{\bar{\bar{\gamma}}_2} F_{\gamma_2}(\gamma)d\gamma\right) \tag{4.123}$$

Substituting $F_{\gamma_2}(\gamma)$ in equation (4.47) into equation (4.123)

$$\mathcal{E}_2 = \bar{\mathcal{E}}_2 + \theta_2\sqrt{m}\left(\int_{\bar{\gamma}_2}^{\bar{\beta}} 1 - \exp\left(-\frac{N_0\gamma}{P\Omega_2(\beta_2 - \beta_1\gamma)}\right)d\gamma + \int_{\bar{\beta}}^{\bar{\bar{\gamma}}_2} 1 d\gamma\right) \tag{4.124}$$

$$= \bar{\mathcal{E}}_2 + \theta_2\sqrt{m}(\bar{\bar{\gamma}}_2 - \bar{\gamma}_2) - \theta_2\sqrt{m}\int_{\bar{\gamma}_2}^{\bar{\beta}} \exp\left(-\frac{N_0\gamma}{P\Omega_2(\beta_2 - \beta_1\gamma)}\right)d\gamma \tag{4.125}$$

Substituting $\bar{\bar{\gamma}}_2$ in equation (4.89) and $\bar{\gamma}_2$ in equation (4.88) into equation (4.125)

$$\mathcal{E}_2 = \bar{\mathcal{E}}_2 + 1 - \theta_2\sqrt{m}\int_{\bar{\gamma}_2}^{\bar{\beta}} \exp\left(-\frac{N_0\gamma}{P\Omega_2(\beta_2 - \beta_1\gamma)}\right)d\gamma \tag{4.126}$$

$$\begin{aligned} = \bar{\mathcal{E}}_2 + 1 &+ \theta_2\sqrt{m}\left(\frac{1}{\frac{N_0\Omega_2 P\beta_2}{(\Omega_2 P(\beta_2 - \beta_1\bar{\beta}))^2}}\exp(-\frac{N_0\bar{\beta}}{P\Omega_2(\beta_2 - \beta_1\bar{\beta})})\right) \\ &+ \theta_2\sqrt{m}\left(\frac{1}{\frac{N_0\Omega_2 P\beta_2}{(\Omega_2 P(\beta_2 - \beta_1\bar{\gamma}_2))^2}}\exp(-\frac{N_0\bar{\gamma}_2}{P\Omega_2(\beta_2 - \beta_1\bar{\gamma}_2)})\right) \end{aligned} \tag{4.127}$$

Case $\bar{\beta} \geq \bar{\bar{\gamma}}_2$

$$\mathcal{E}_2 = \bar{\mathcal{E}}_2 + \theta_2\sqrt{m}\int_{\bar{\gamma}_2}^{\bar{\bar{\gamma}}_2} F_{\gamma_2}(\gamma)d\gamma \tag{4.128}$$

Substituting $F_{\gamma_2}(\gamma)$ for $\gamma \leq \bar{\beta}$ in equation (4.36) into equation (4.128)

$$\mathcal{E}_2 = \bar{\mathcal{E}}_2 + \theta_2\sqrt{m}\int_{\bar{\gamma}_2}^{\bar{\bar{\gamma}}_2} 1 - \exp\left(-\frac{N_0\gamma}{P\Omega_2(\beta_2 - \beta_1\gamma)}\right)d\gamma \tag{4.129}$$

$$\begin{aligned} = \bar{\mathcal{E}}_2 + 1 &+ \frac{\theta_2\sqrt{m}}{\frac{N_0\Omega_2 P\beta_2}{(\Omega_2 P(\beta_2 - \beta_1\bar{\bar{\gamma}}_2))^2}}\exp(-\frac{N_0\bar{\bar{\gamma}}_2}{P\Omega_2(\beta_2 - \beta_1\bar{\bar{\gamma}}_2)}) \\ &+ \frac{\theta_2\sqrt{m}}{\frac{N_0\Omega_2 P\beta_2}{(\Omega_2 P(\beta_2 - \beta_1\bar{\gamma}_2))^2}}\exp(-\frac{N_0\bar{\gamma}_2}{P\Omega_2(\beta_2 - \beta_1\bar{\gamma}_2)}) \end{aligned} \tag{4.130}$$

Combining equations (4.123), (4.127) and (4.130), $\mathcal{E}_2$ can be expressed as

$$\mathcal{E}_2 = \begin{cases} \bar{\mathcal{E}}_2 + 1 & \bar{\beta} < \bar{\gamma_2} \\ \bar{\mathcal{E}}_2 + 1 + \theta_2\sqrt{m}\left(\frac{1}{\frac{N_0\Omega_2 P\beta_2}{(\Omega_2 P(\beta_2-\beta_1\bar{\beta}))^2}}\exp(-\frac{N_0\bar{\beta}}{P\Omega_2(\beta_2-\beta_1\bar{\beta})})\right) \\ \quad +\theta_2\sqrt{m}\left(\frac{1}{\frac{N_0\Omega_2 P\beta_2}{(\Omega_2 P(\beta_2-\beta_1\bar{\gamma_2}))^2}}\exp(-\frac{N_0\bar{\gamma_2}}{P\Omega_2(\beta_2-\beta_1\bar{\gamma_2})})\right) & \bar{\gamma_2} \le \bar{\beta} < \bar{\bar{\gamma_2}} \\ \bar{\mathcal{E}}_2 + 1 + \theta_2\sqrt{m}\left(\frac{1}{\frac{N_0\Omega_2 P\beta_2}{(\Omega_2 P(\beta_2-\beta_1\bar{\bar{\gamma_2}}))^2}}\exp(-\frac{N_0\bar{\bar{\gamma_2}}}{P\Omega_2(\beta_2-\beta_1\bar{\bar{\gamma_2}})}\right) \\ \quad +\theta_2\sqrt{m}\left(\frac{1}{\frac{N_0\Omega_2 P\beta_2}{(\Omega_2 P(\beta_2-\beta_1\bar{\gamma_2}))^2}}\exp(-\frac{N_0\bar{\gamma_2}}{P\Omega_2(\beta_2-\beta_1\bar{\gamma_2})})\right) & \bar{\beta} \ge \bar{\bar{\gamma_2}} \end{cases} \tag{4.131}$$

$\Omega_2 = d_2^{-n}$. Where d_2 is distance from BS to UE_2 and n is Path loss exponent.

The BLER when EV decodes UE_1 signal can be evaluated evaluated as

$$\mathcal{E}_3 = \bar{\mathcal{E}}_3 + \theta_3\sqrt{m}\int_{\bar{\gamma_3}}^{\bar{\bar{\gamma_3}}} F_{\gamma_{E,1}}(\gamma)d\gamma \tag{4.132}$$

Case $\bar{\beta} < \bar{\gamma_3}$

$$\mathcal{E}_3 = \bar{\mathcal{E}}_3 + \theta_3\sqrt{m}\int_{\bar{\gamma_3}}^{\bar{\bar{\gamma_3}}} F_{\gamma_{E,1}}(\gamma)d\gamma \tag{4.133}$$

$$= \bar{\mathcal{E}}_3 + 1 \tag{4.134}$$

Case $\bar{\gamma_3} \le \bar{\beta} < \bar{\bar{\gamma_3}}$

$$\mathcal{E}_3 = \bar{\mathcal{E}}_3 + \theta_3\sqrt{m}\left(\int_{\bar{\gamma_3}}^{\bar{\beta}} F_{\gamma_{E,1}}(\gamma)d\gamma + \int_{\bar{\beta}}^{\bar{\bar{\gamma_3}}} F_{\gamma_{E,1}}(\gamma)d\gamma\right) \tag{4.135}$$

$$\begin{aligned} &= \bar{\mathcal{E}}_3 + 1 + \frac{\theta_3\sqrt{m}}{\frac{N_0}{\beta_1\Omega_1 P} + \frac{N_0\Omega_2 P\beta_2}{(\Omega_2 P(\beta_2-\beta_1\bar{\beta}))^2}}\exp\left(\frac{-N_0\bar{\beta}}{\beta_1\Omega_1 P} - \frac{N_0\bar{\beta}}{P\Omega_2(\beta_2-\beta_1\bar{\beta})}\right) \\ &\quad + \frac{\theta_3\sqrt{m}}{\frac{N_0}{\beta_1\Omega_1 P} + \frac{N_0\Omega_2 P\beta_2}{(\Omega_2 P(\beta_2-\beta_1\bar{\gamma_3}))^2}}\exp\left(\frac{-N_0\bar{\gamma_3}}{\beta_1\Omega_1 P} - \frac{N_0\bar{\gamma_3}}{P\Omega_2(\beta_2-\beta_1\bar{\gamma_3})}\right) \end{aligned} \tag{4.136}$$

Case $\bar{\beta} \ge \bar{\bar{\gamma_3}}$

$$\mathcal{E}_3 = \bar{\mathcal{E}}_3 + \theta_3\sqrt{m}\int_{\bar{\beta}}^{\bar{\bar{\gamma_3}}} F_{\gamma_{E,1}}(\gamma)d\gamma \tag{4.137}$$

$$\begin{aligned} &= \bar{\mathcal{E}}_3 + 1 - \frac{\theta_3\sqrt{m}}{\frac{N_0}{\beta_1\Omega_1 P} + \frac{N_0\Omega_2 P\beta_2}{(\Omega_2 P(\beta_2-\beta_1\bar{\bar{\gamma_3}}))^2}}\exp\left(\frac{-N_0\bar{\bar{\gamma_3}}}{\beta_1\Omega_1 P} - \frac{N_0\bar{\bar{\gamma_3}}}{P\Omega_2(\beta_2-\beta_1\bar{\bar{\gamma_3}})}\right) \\ &\quad + \frac{\theta_3\sqrt{m}}{\frac{N_0}{\beta_1\Omega_1 P} + \frac{N_0\Omega_2 P\beta_2}{(\Omega_2 P(\beta_2-\beta_1\bar{\beta}))^2}}\exp\left(\frac{-N_0\bar{\beta}}{\beta_1\Omega_1 P} - \frac{N_0\bar{\beta}}{P\Omega_2(\beta_2-\beta_1\bar{\beta})}\right) \end{aligned} \tag{4.138}$$

Combining equations (4.134), (4.136) and (4.138)$\mathcal{E}_1$ can be expressed as

$$\mathcal{E}_3 = \begin{cases} \bar{\mathcal{E}}_3 + 1 & \bar{\beta} < \bar{\gamma_3} \\ \bar{\mathcal{E}}_3 + 1 + \frac{\theta_3\sqrt{m}}{\frac{N_0}{\beta_1\Omega_1 P} + \frac{N_0\Omega_2 P\beta_2}{(\Omega_2 P(\beta_2-\beta_1\bar{\beta}))^2}} \exp\left(\frac{-N_0\bar{\beta}}{\beta_1\Omega_1 P} - \frac{N_0\bar{\beta}}{P\Omega_2(\beta_2-\beta_1\bar{\beta})}\right) & \\ \quad + \frac{\theta_3\sqrt{m}}{\frac{N_0}{\beta_1\Omega_1 P} + \frac{N_0\Omega_2 P\beta_2}{(\Omega_2 P(\beta_2-\beta_1\bar{\gamma_3}))^2}} \exp\left(\frac{-N_0\bar{\gamma_3}}{\beta_1\Omega_1 P} - \frac{N_0\bar{\gamma_3}}{P\Omega_2(\beta_2-\beta_1\bar{\gamma_3})}\right) & \bar{\gamma_3} \le \bar{\beta} < \bar{\bar{\gamma_3}} \\ \bar{\mathcal{E}}_3 + 1 - \frac{\theta_3\sqrt{m}}{\frac{N_0}{\beta_1\Omega_1 P} + \frac{N_0\Omega_2 P\beta_2}{(\Omega_2 P(\beta_2-\beta_1\bar{\bar{\gamma_3}}))^2}} \exp\left(\frac{-N_0\bar{\bar{\gamma_3}}}{\beta_1\Omega_1 P} - \frac{N_0\bar{\bar{\gamma_3}}}{P\Omega_2(\beta_2-\beta_1\bar{\bar{\gamma_3}})}\right) & \\ \quad + \frac{\theta_3\sqrt{m}}{\frac{N_0}{\beta_1\Omega_1 P} + \frac{N_0\Omega_2 P\beta_2}{(\Omega_2 P(\beta_2-\beta_1\bar{\beta}))^2}} \exp\left(\frac{-N_0\bar{\beta}}{\beta_1\Omega_1 P} - \frac{N_0\bar{\beta}}{P\Omega_2(\beta_2-\beta_1\bar{\beta})}\right) & \bar{\beta} \ge \bar{\bar{\gamma_3}} \end{cases} \tag{4.139}$$

The BLER when EV decodes UE_2 signal can be evaluated as

$$\mathcal{E}_4 = \bar{\mathcal{E}}_4 + \theta_4\sqrt{m}\int_{\bar{\gamma_4}}^{\bar{\bar{\gamma_4}}} F_{\gamma_{E,2}}(\gamma)d\gamma \tag{4.140}$$

Case $\bar{\beta} < \bar{\gamma_4}$

$$\mathcal{E}_4 = \bar{\mathcal{E}}_4 + \theta_4\sqrt{m}\int_{\bar{\gamma_4}}^{\bar{\bar{\gamma_4}}} F_{\gamma_{E,2}}(\gamma)d\gamma \tag{4.141}$$

$$= \bar{\mathcal{E}}_4 + 1 \tag{4.142}$$

Case $\bar{\gamma_4} \le \bar{\beta} < \bar{\bar{\gamma_4}}$

$$\mathcal{E}_4 = \bar{\mathcal{E}}_4 + \theta_4\sqrt{m}\left(\int_{\bar{\gamma_4}}^{\bar{\beta}} F_{\gamma_{E,2}}(\gamma)d\gamma + \int_{\bar{\beta}}^{\bar{\bar{\gamma_4}}} F_{\gamma_{E,2}}(\gamma)d\gamma\right) \tag{4.143}$$

$$\begin{aligned} &= \bar{\mathcal{E}}_4 + 1 + \frac{\theta_4\sqrt{m}}{\frac{N_0\Omega_3 P\beta_2}{(\Omega_3 P(\beta_2-\beta_1\bar{\beta}))^2}} \exp(-\frac{N_0\bar{\beta}}{P\Omega_3(\beta_2-\beta_1\bar{\beta})}) \\ &\quad + \frac{\theta_4\sqrt{m}}{\frac{N_0\Omega_3 P\beta_2}{(\Omega_3 P(\beta_2-\beta_1\bar{\gamma_4}))^2}} \exp(-\frac{N_0\bar{\gamma_4}}{P\Omega_3(\beta_2-\beta_1\bar{\gamma_4})}) \end{aligned} \tag{4.144}$$

Case $\bar{\beta} \ge \bar{\bar{\gamma_4}}$

$$\mathcal{E}_4 = \bar{\mathcal{E}}_4 + \theta_4\sqrt{m}\int_{\bar{\beta}}^{\bar{\bar{\gamma_4}}} F_{\gamma_{E,2}}(\gamma)d\gamma \tag{4.145}$$

$$\begin{aligned} &= \bar{\mathcal{E}}_4 + 1 + \theta_4\sqrt{m}\left(\frac{1}{\frac{N_0\Omega_3 P\beta_2}{(\Omega_3 P(\beta_2-\beta_1\bar{\bar{\gamma_4}}))^2}} \exp(-\frac{N_0\bar{\bar{\gamma_4}}}{P\Omega_3(\beta_2-\beta_1\bar{\bar{\gamma_4}})})\right) \\ &\quad + \theta_4\sqrt{m}\left(\frac{1}{\frac{N_0\Omega_3 P\beta_2}{(\Omega_3 P(\beta_2-\beta_1\bar{\beta}))^2}} \exp(-\frac{N_0\bar{\beta}}{P\Omega_3(\beta_2-\beta_1\bar{\beta})})\right) \end{aligned} \tag{4.146}$$

Combining (4.142), (4.144) and (4.146), $\mathcal{E}_4$ can be expressed as

$$\mathcal{E}_4 = \begin{cases} \bar{\mathcal{E}}_4 + 1 & \bar{\beta} < \bar{\gamma_3} \\ \bar{\mathcal{E}}_4 + 1 + \theta_4\sqrt{m}\left(\frac{1}{\frac{N_0\Omega_3 P\beta_2}{(\Omega_3 P(\beta_2-\beta_1\bar{\beta}))^2}}\exp(-\frac{N_0\bar{\beta}}{P\Omega_3(\beta_2-\beta_1\bar{\beta})})\right) \\ \quad +\theta_4\sqrt{m}\left(\frac{1}{\frac{N_0\Omega_3 P\beta_2}{(\Omega_3 P(\beta_2-\beta_1\bar{\gamma_4}))^2}}\exp(-\frac{N_0\bar{\gamma_4}}{P\Omega_3(\beta_2-\beta_1\bar{\gamma_4})})\right) & \bar{\gamma_3} \leq \bar{\beta} < \bar{\bar{\gamma_3}} \\ \bar{\mathcal{E}}_4 + 1 + \theta_4\sqrt{m}\left(\frac{1}{\frac{N_0\Omega_3 P\beta_2}{(\Omega_3 P(\beta_2-\beta_1\bar{\bar{\gamma_4}}))^2}}\exp(-\frac{N_0\bar{\bar{\gamma_4}}}{P\Omega_3(\beta_2-\beta_1\bar{\bar{\gamma_4}})})\right) \\ \quad +\theta_4\sqrt{m}\left(\frac{1}{\frac{N_0\Omega_3 P\beta_2}{(\Omega_3 P(\beta_2-\beta_1\bar{\beta}))^2}}\exp(-\frac{N_0\bar{\beta}}{P\Omega_3(\beta_2-\beta_1\bar{\beta})})\right) & \bar{\beta} \geq \bar{\bar{\gamma_3}} \end{cases} \tag{4.147}$$

4.3.2 Secrecy Capacity

Secrecy capacity ($\bar{C_i}$) can be achieved by subtracting Shannon capacity at EV ($R_{E,i}$) from Shannon capacity at UE_i ($\bar{R_i}$). Mathematically, it can be evaluated as

$$\bar{C_i} = \bar{R_i} - \bar{R}_{E,i} \tag{4.148}$$

Instantaneous Capacity of UE_i can be evaluated as

$$R_i(\gamma_i) = B\log_2(1+\gamma) - \sqrt{\frac{\vartheta(\gamma)}{n_i}}Q^{-1}(\mathcal{E}_i) \tag{4.149}$$

Where $\log_2(1+\gamma)$ represents conventional Shannon capacity, $\vartheta(\gamma)$ represents channel dispersion at γ_i for infinite block length n_i and B is the bandwidth of the channel (Hz). $\vartheta(\gamma)$ can be evaluated as

$$\vartheta(\gamma) = 1 - (1+\gamma)^{-}2 \tag{4.150}$$

$$= \frac{\gamma^2+2\gamma}{(1+\gamma)^2} \tag{4.151}$$

Substituting equation (4.151) into (4.149)

$$R_i(\gamma_i) = B\log_2(1+\gamma) - \sqrt{\frac{\gamma^2+2\gamma}{n_i(1+\gamma)^2}}Q^{-1}(\mathcal{E}_i) \tag{4.152}$$

Where, $Q^{-1}(\mathcal{E}_i)$ represents reserve Gaussian Q-function at $\mathcal{E}_i$ and can be evaluated as

$$Q(\mathcal{E}_i) = \frac{1}{\sqrt{2\pi}}\int_{\mathcal{E}_i}^{\infty}\exp(-\frac{u^2}{2})du \tag{4.153}$$

Substituting equation (4.153) into equation (4.152)

$$R_i = \int_0^{\infty}\left[B\log_2(1+\gamma) - \log_2(e)\sqrt{\frac{\gamma^2+2\gamma}{n_i(1+\gamma)^2}}Q^{-1}(\mathcal{E}_i)\right]f\gamma_i(\gamma)d\gamma \tag{4.154}$$

$$\bar{R}_i = \int_0^\infty B\log_2(1+\gamma) f\gamma_i(\gamma)d\gamma - \log_2(e)Q^{-1}(\mathcal{E}_i)\int_0^\infty \sqrt{\frac{\gamma^2+2\gamma}{n_i(1+\gamma)^2}} f\gamma_i(\gamma)d\gamma \quad (4.155)$$

Shannon Capacity at UE_1 can be evaluated as

$$\begin{aligned}\bar{R}_1 = &\int_0^\infty B\log_2(1+\gamma) f\gamma_1(\gamma)d\gamma \\ &- \log_2(e)Q^{-1}(\mathcal{E}_1)\int_0^\infty \sqrt{\frac{\gamma^2+2\gamma}{n_1(1+\gamma)^2}} f\gamma_1(\gamma)d\gamma\end{aligned} \quad (4.156)$$

Shannon Capacity at UE_2 can be evaluated as

$$\begin{aligned}\bar{R}_2 = &\int_0^\infty B\log_2(1+\gamma) f\gamma_2(\gamma)d\gamma \\ &- \log_2(e)Q^{-1}(\mathcal{E}_2)\int_0^\infty \sqrt{\frac{\gamma^2+2\gamma}{n_2(1+\gamma)^2}} f\gamma_2(\gamma)d\gamma\end{aligned} \quad (4.157)$$

Shannon Capacity at EV with UE_1 signal can be evaluated as

$$\begin{aligned}\bar{R}_{E,1} = &\int_0^\infty \log_2(1+\gamma) f\gamma_{E,1}(\gamma)d\gamma \\ &- \log_2(e)Q^{-1}(\mathcal{E}_3)\int_0^\infty \sqrt{\frac{\gamma^2+2\gamma}{n_3(1+\gamma)^2}} f\gamma_{E,1}(\gamma)d\gamma\end{aligned} \quad (4.158)$$

Shannon Capacity at EV with UE_2 signal can be evaluated as

$$\begin{aligned}\bar{R}_{E,2} = &\int_0^\infty \log_2(1+\gamma) f\gamma_{E,2}(\gamma)d\gamma \\ &- \log_2(\exp)Q^{-1}(\mathcal{E}_4)\int_0^\infty \sqrt{\frac{\gamma^2+2\gamma}{n_4(1+\gamma)^2}} f\gamma_{E,2}(\gamma)d\gamma\end{aligned} \quad (4.159)$$

Secrecy Capacity of UE_1 and UE_2 can be evaluated as

$$\bar{C}_1 = \bar{R}_1 - \bar{R}_{E,1} \quad (4.160)$$

$$\bar{C}_2 = \bar{R}_2 - \bar{R}_{E,2} \quad (4.161)$$

Chapter 5

Results and Discussion

The primary objective of this study was to evaluate the performance of NOMA system within the realm of PLS, focusing on SPC. This chapter presents the findings and discussion of key performance metrics, CDF, BLER, and secrecy capacity, in the context of NOMA's application within wireless communication systems.

The NOMA system's setup includes a BS, two users, and an EV. The metrics chosen for analysis were carefully selected to provide insights into the reliability, security, and capacity of the system under varying conditions.

The methodology adopted for this analysis involved rigorous mathematical calculations and MATLAB generated graphical representations. By leveraging mathematical models and numerical computations. The analysis incorporated realistic channel conditions, power allocation strategies, and pertinent system parameters to emulate real-world scenarios accurately.

The findings presented in this chapter aim to present a comprehensive evaluation of NOMA's efficacy in achieving robust security measures while facilitating efficient short packet transmissions. Furthermore, the discussion of these results will provide valuable insights into the practical implications of NOMA systems in real-world deployment scenarios.

5.1 Cumulative Distribution Function

The CDF of the SINR values for UE_1 and UE_2 within the NOMA system was derived through meticulous mathematical computations. Specifically, Equations (4.36) and (4.47) were employed to drive the CDF for UE_1 and UE_2 respectively.

Graphs depicting the SINR were generated using MATLAB to visualize the system's performance. The generation of these graphs involved a meticulous selection of parameters that influence the wireless communication environment. The parameters used in the graph generation were carefully chosen to simulate realistic conditions and comprehend the behavior of the NOMA system under varying scenarios.

The main parameters involved in the setup were, noise power spectral density ($N0$), representing the inherent noise in the system. Total power (P), indicative of the overall power available for transmission. Path loss exponent (n), affecting signal attenuation over distance. Power channel gains (Ω_1), representing the power received at each user considering distance based attenuation. Power allocation coefficients ($\beta_1 \& \beta_2$) to determining the power allocation among users based on their channel gains and SINR, providing insights into performance across various signal strength scenarios.

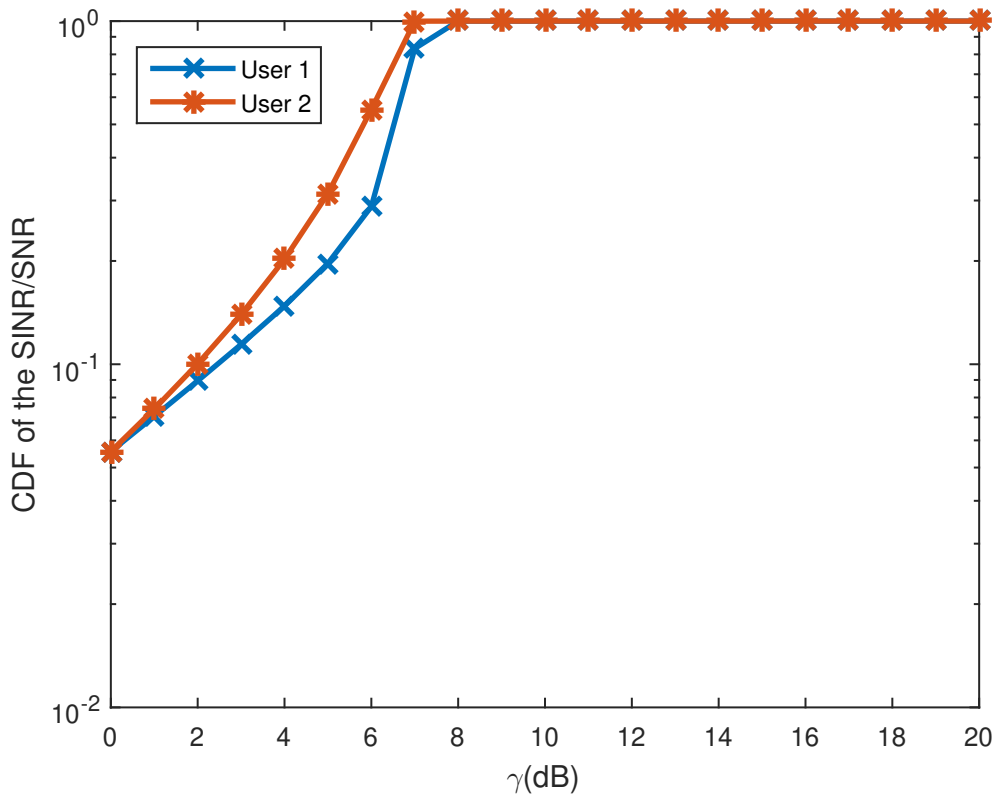

Figure 5.1: CDF of SINR

Figure 5.1 shows CDF of the SINR values for both users. The CDF analysis provides a comprehensive understanding of the probability distribution of SINR values for the individual users within the NOMA setup. By utilizing established mathematical formulations, this analysis facilitates the characterization of the likelihood of attaining specific SINR levels for each user in the system.

As seen in Figure 5.1 as γ increases from 0dB to 8dB, CDF of the SINR/SNR increases. This increase signifies an increasing likelihood of achieving higher SINR/SNR values, indicative of improved signal quality and reduced interference within the system. However, when $\gamma > 8$, CDF of the SINR/SNR remains constant at 1, which implies that beyond this threshold, the likelihood of achieving higher SINR/SNR values becomes constant, suggesting a limit to the achievable performance within the considered system parameters.

In essence, the CDF serves as a fundamental metric illuminating the statistical distribution of SINR/SNR values. Its portrayal of the cumulative probability provides a crucial lens through which to comprehend the variability and reliability inherent in the communication channels of the NOMA system.

5.2 Block Error Rate of Users with Fixed Path Loss Exponent

The BLER assessment for UE_1 and UE_2 involved a meticulous approach utilizing specific equations, (4.116) and (4.131), tailored to derive BLER values at each user in the NOMA system. These equations were derived by integrating the CDF as part of the methodology to calculate BLER for each user.

For visual representation and deeper comprehension, MATLAB was employed to generate graphs illustrating the BLER. This process entailed a thoughtful selection of parameters that influence the wireless communication environment.

The main parameters involved in the setup were, distance from BS to users, to examine how distance affects BLER. Data block size, to examine the effect of transmitted data size on BLER. Channel use, to examine the effect of the channel on use on BLER. Path loss exponent, to examine the effect of different path lose exponent value on BLER. transmitted signal power, to examine how decreasing or increasing transmitting signal power can affect BLER with in the NOMA system setup..

The BLER serves as a pivotal metric in assessing error probabilities within data blocks. Figure 5.2 delineates distinct BLER trends within 100-bit data blocks for UE_1 and UE_2 considering a set channel use of 2000. While considering an identical path loss exponent for both users, the distinct BLER observed within the same data blocks for these users with in the NOMA setup is primarily influenced by their differing distances from the BS.

UE_2 being situated farther from the BS experiences a comparatively higher BLER due to increased distance. Despite the consistent path loss exponent, the longer propagation path for UE_2 results in a reduced received power compared to UE_1. Consequently, UE_2 encounters a relatively lower received signal power, affecting SINR.

With a diminished SINR, UE_2 becomes more susceptible to the effects of noise, interference, and fading despite the consistent path loss exponent. This increased vulnerability translates into a higher probability of errors within the same data block size, thereby leading to a higher BLER for UE_2 compared to UE_1

Hence, even with an equivalent path loss exponent, the spatial separation between users and the BS influences received signal strength, impacting SNR and subsequently, the observed BLER. This emphasizes the critical role of user proximity to the BS in affecting error rates within NOMA systems, especially when considering consistent path loss exponents.

Another notable trend observed from Figure 5.2 is the consistent decrease in BLER for both users as the transmitted SINR/SNR increases. This trend holds significance when considering consistent factors such as data packet size, path loss exponent, and channel use. The consistent reduction in BLER despite maintaining identical parameters affirms the pivotal role of transmitted signal power in influencing BLER within the NOMA system. As the SNR/SINR escalates from 0dB to 10dB due to increased transmitted signal power, the received signal strength at both users proportionally improves.

With a higher SINR/SNR, the susceptibility to interference and noise diminishes, resulting in a decreased probability of errors occurring within the transmitted data

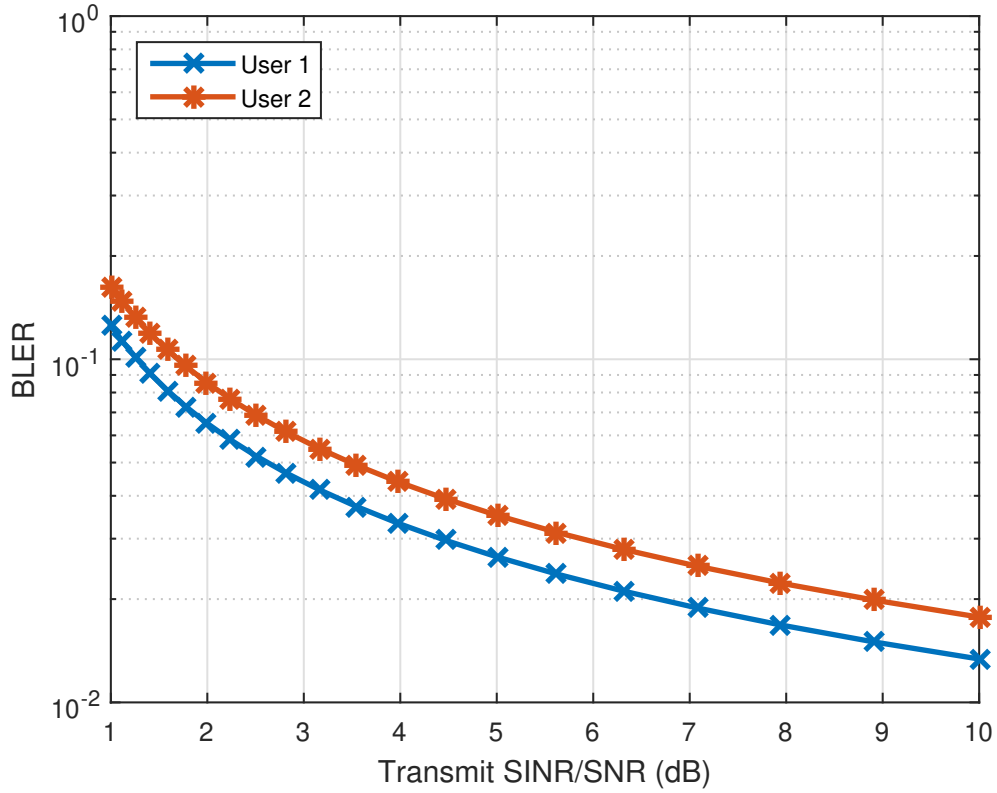

Figure 5.2: BLER of Users

packets. The observed decline in BLER across both users underscores the positive correlation between transmitted SINR/SNR and error reduction. This consistency in the trend, while keeping parameters constant, emphasizes the reliability and predictability of the relationship between signal power and error performance within NOMA systems. Understanding this relationship is pivotal in system optimization, particularly in regulating transmitted signal power to achieve desired error performance, especially in scenarios demanding high reliability for SPC.

In essence, the observed reduction in BLER as transmitted SINR/SNR increases reaffirms the significance of sufficient signal strength in ensuring reliable data transmission, regardless of consistent factors like data packet size, path loss exponent, and channel use.

5.3 Secrecy Capacity of Users with Fixed Path Loss Exponent

The secrecy capacity assessment for UE_1 and UE_2 involved a meticulous approach utilizing specific equations, (4.160) and (4.161), tailored to derive secrecy capacity values at each user in the NOMA system. These equations were derived by deriving instantaneous capacity of UE_1, UE_2 and EV which further involved calculating the Q-function of the instantaneous BLER and integrating the PDF as part of the methodology to calculate secrecy capacity for each user.

For visual representation and deeper comprehension, MATLAB was employed to generate graphs illustrating the secrecy capacity. This process entailed a thoughtful selection of parameters that influence the wireless communication environment.

The main parameters involved in the setup were, distance from BS to users, to examine how distance affects secrecy capacity, data block size, to examine the effect of transmitted data size on secrecy capacity. Channel, to examine the effect of the channel on use on secrecy capacity. Path loss exponent, to examine the effect of different path lose exponent value on secrecy capacity. transmitted signal power, to examine how decreasing or increasing transmitting signal power can affect secrecy capacity within the NOMA setup.

Secrecy capacity helps assess the level of security in communication systems. It quantifies the maximum rate at which information can be reliably transmitted between legitimate users while keeping it confidential from eavesdroppers.

The distinct trends in secrecy capacity observed within 100-bit data blocks for UE_1 and UE_2, as depicted in Figure 5.3, are influenced by their respective distances from the BS in the NOMA setup. Despite assuming an identical path loss exponent for both users, the disparity in secrecy capacity within these data blocks primarily arises from the users' differing distances from the BS.

The varying distances introduce distinct channel conditions for UE_1 and UE_2, consequently impacting their received signal strengths. As a result, the achievable secrecy capacity exhibits marked differences. Closer proximity to the BS generally affords stronger received signal power, leading to relatively higher secrecy capacity due to improved SNR and reduced interference from potential eavesdroppers.

Furthermore, while maintaining a fixed channel use, data block size and path loss exponent, the distinct trends in secrecy capacity shown in Figure 5.3 presents an opportunity to delve deeper into optimizing system performance while ensuring secure communication channels for users at varying distances.

In essence, the distinct secrecy capacity trends witnessed in the NOMA system for UE_1 and UE_2 underscore the critical influence of user proximity to the BS on the achievable secrecy capacity. Understanding these variations not only informs system design but also highlights the trade-offs between user distances, received signal strengths, and resultant secrecy capacity in SPC.

The consistent increase in secrecy capacity observed for both users in Figure 5.3, aligned with escalating transmitted SINR/SNR, reveals a pivotal relationship between transmitted signal power and information confidentiality within the NOMA system. This trend remains consistent, holding significance even when maintaining factors such as data packet size, path loss exponent, and channel use constant.

The escalation of transmitted SINR/SNR from 0dB to 10dB, attributing to increased transmitted signal power, directly correlates with an improvement in received signal strength at both users. This rise in signal strength diminishes susceptibility to interference and noise, resulting in a noticeable boost in secrecy capacity. It underscores the positive and proportional relationship between transmitted SINR/SNR and the system's ability to maintain secure communication channels

This consistent trend underlines the reliability and predictability of the relationship between signal power and information confidentiality within NOMA systems. Understanding this linkage is pivotal for system optimization, especially concerning the regulation of transmitted signal power to achieve desired secrecy capacity. This is

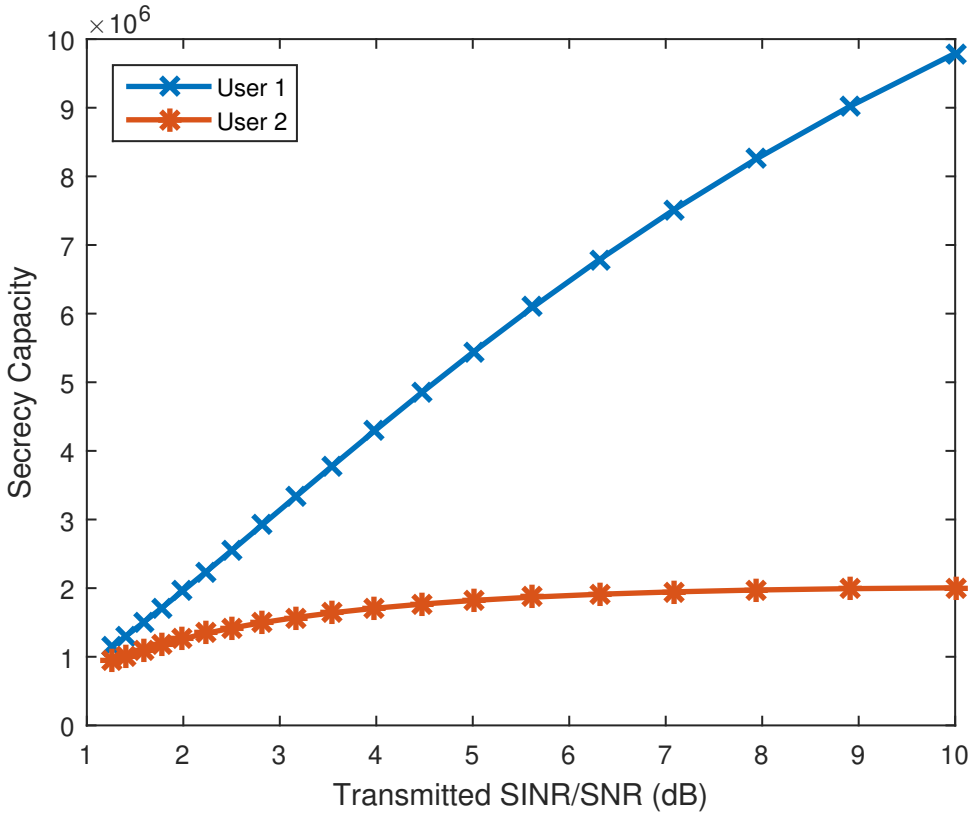

Figure 5.3: Secrecy Capacity of Users

particularly pertinent in scenarios demanding high reliability for SPC or applications requiring robust security protocols.

In practical application, such as scenarios involving sensitive data transmission or critical communication, leveraging this understanding becomes paramount. It enables the design of optimized strategies for power allocation, adaptive modulation techniques, or resource allocation within the NOMA framework to strike a balance between secrecy capacity, system efficiency, and reliable data transmission.

In essence, the consistent elevation in secrecy capacity with escalating transmitted SINR/SNR reaffirms the vital role of sufficient signal strength in guaranteeing reliable and secure data transmission. By recognizing this relationship, NOMA systems can achieve heightened security and efficiency across various applications and operational environments.

5.4 Average Block Error Rate with Varying Path Loss Exponent Values

The path loss exponent determines how fast the signal power diminishes with distance. A higher path loss exponent signifies a more rapid decrease in signal power with distance, while a lower path loss exponent indicates slower attenuation.

Figure 5.4 shows average BLER for UE_1 and UE_2 across varying path loss exponent values ($n = 2, 3, 4, 5$). The trend indicates that as the path loss exponent

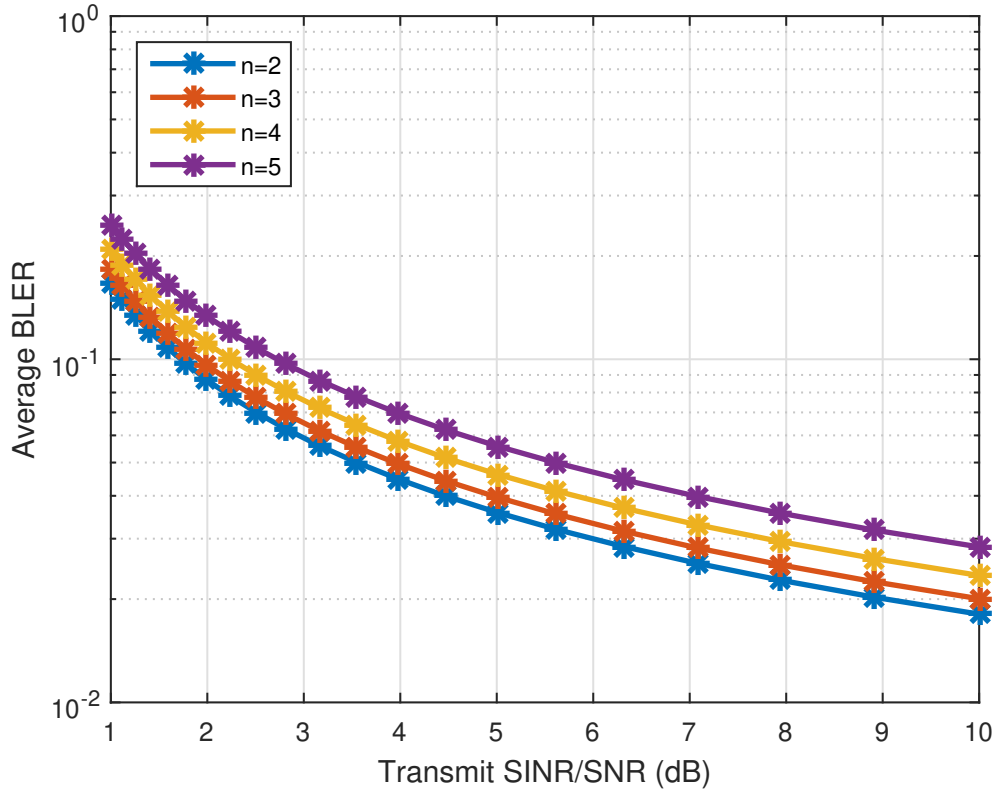

Figure 5.4: Average BLER with Varying Path Loss Exponent

increases from lower values ($n = 2$) to higher values ($n = 5$), the average BLER demonstrates a consistent increase. This corresponds to the interplay between path loss exponent and the SINR/SNR.

A higher path loss exponent signifies a more aggressive attenuation of the transmitted signal over distance. Consequently, in scenarios where path loss exponent is higher, the received signal strength relative to interference and noise diminishes considerably. This results in a lower SINR/SNR, leading to higher average BLER values as decoding accuracy is impacted by the weakened received signal.

Conversely, lower path loss exponents as observed at $n = 2$, exhibit slower signal attenuation, allowing the received signal to maintain stronger power even over extended distances. This yields a more favorable SINR/SNR, consequently reducing the average BLER as the robustness of the received signal against interference and noise increases the reliability of data decoding.

In essence, the observed trend with in the specific NOMA setup defies the conventional expectations regarding path loss exponent influence on BLER. It underscores the intricate balance between signal attenuation, interference, noise, and their collective impact on the reliability of communication systems. This understanding is pivotal in optimizing system parameters for increased performance and security in NOMA systems designed for SPC.

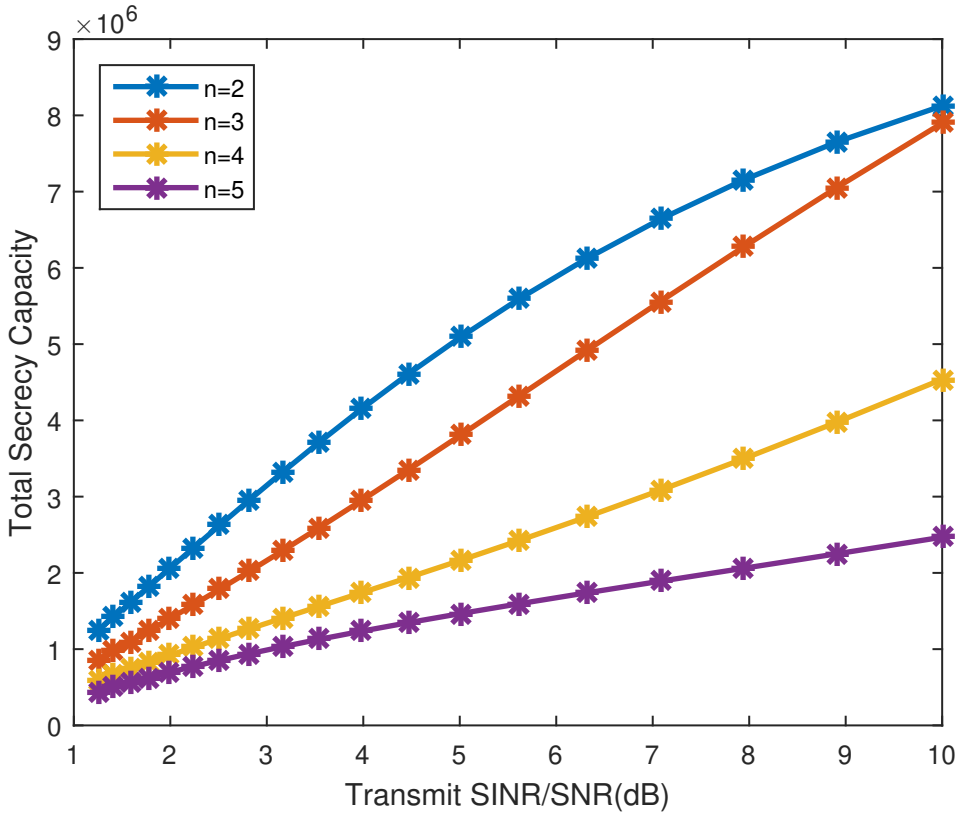

Figure 5.5: Total Secrecy Capacity with Varying Path Loss Exponent

5.5 Total Secrecy Capacity with Varying Path Loss Exponent Values

Figure 5.5 shows total secrecy capacity for UE_1 and UE_2 with varying path loss exponent values ($n = 2, 3, 4, 5$). The trend shows that, as the path loss exponent increases from lower values ($n = 2$) to higher values ($n = 5$), the total secrecy capacity decreases. This shows the inverse relationship between path loss exponent and the SINR/SNR.

A higher path loss exponent signifies a higher attenuation of the transmitted signal over distance. In scenarios where path loss exponent is higher, the received signal strength relative to interference and noise diminishes considerably. This results in lower SINR, leading to lower total secrecy capacity values as decoding accuracy is impacted by the weakened received signal.

Conversely, lower path loss exponents as observed at $n = 2$, exhibit slower signal attenuation, allowing the received signal to maintain stronger power even over extended distances. This yields higher SINR/SNR, consequently increasing the total secrecy capacity as the robustness of the received signal against interference and noise increases the reliability of data decoding. In essence, the observed trend with in the specific NOMA setup defies the conventional expectations regarding path loss exponent influence on secrecy capacity. It underscores the intricate balance between signal attenuation, interference, noise, and their collective impact on the reliability of

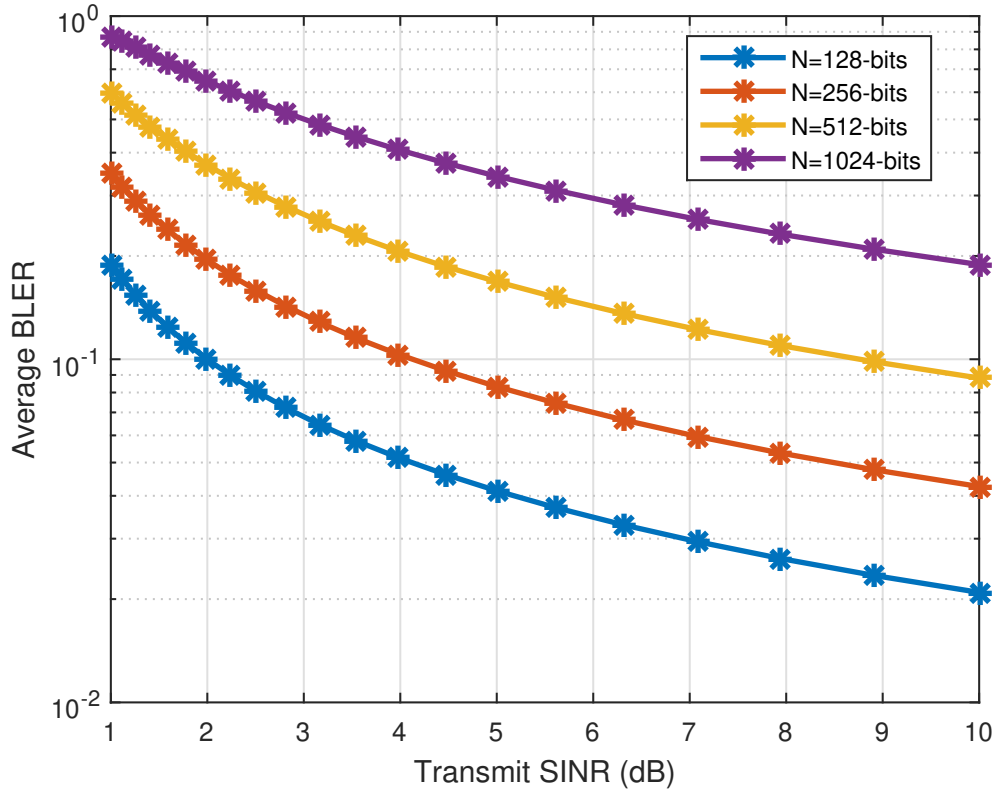

Figure 5.6: Average BLER with Varying Packet Size

communication systems. This understanding is pivotal in optimizing system parameters for increased performance and security in NOMA systems designed for SPC.

5.6 Average Block Error Rate with Different Packet Size

Figure 5.6 illustrates the relationship between average BLER for UE_1 and UE_2 with varying packet sizes. Other parameters such as noise power spectral density ($N0$), Total transmitted power (P), Path loss exponent (n), distance (d), power channel gain (Ω) which is calculated as d^{-n}, channel use (m) and power allocation coefficients ($\beta_1 \& \beta_2$) are used to calculate the average BLER. The observed trend indicates that as the packet size increases, the average BLER also increases. A larger packet size implies the transmission of a greater amount of data within each packet. During transmission, any error affecting even a single bit within the larger packet renders the entire packet erroneous. Therefore, larger packets are more susceptible to errors as compared to smaller ones due to the increased likelihood of encountering channel impairments during transmission.

Hence, the increase in average BLER with larger packet sizes is primarily attributed to the heightened susceptibility of larger packets to transmission errors, which subsequently impairs the received signal quality, impacting the accurate de-

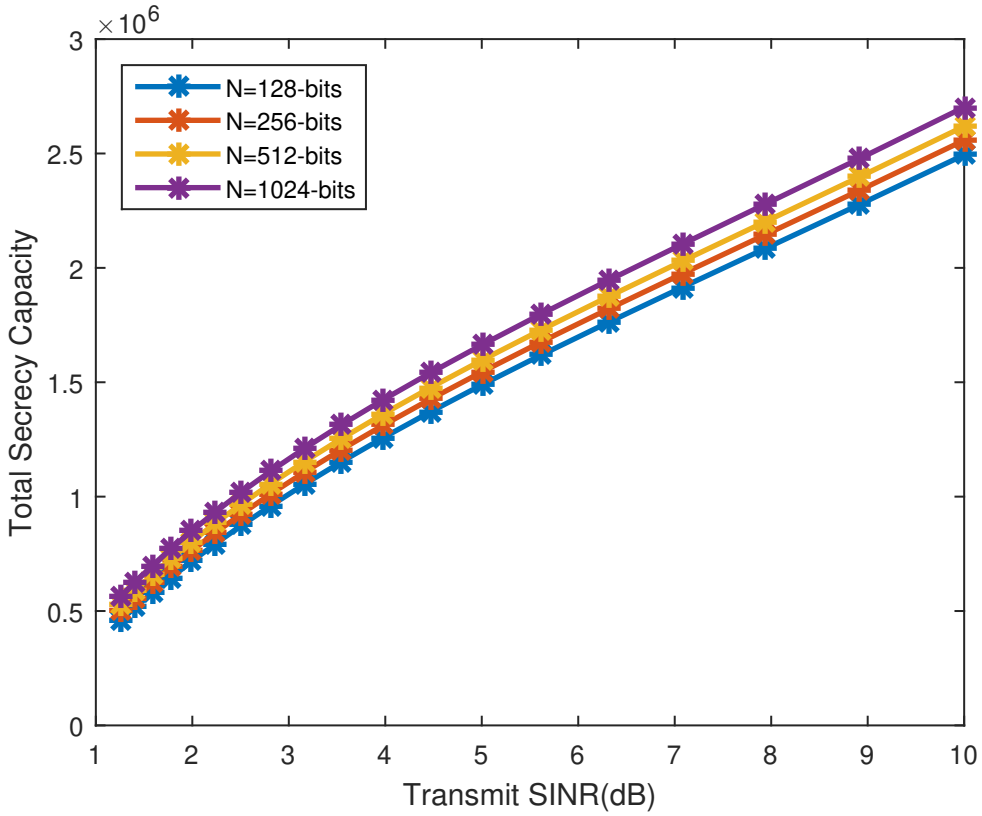

Figure 5.7: Total Secrecy capacity with Varying Packet Size

coding of the entire packet.

5.7 Total Secrecy Capacity with Different Packet Size

Figure 5.7 illustrates the total secrecy capacity for UE_1 and UE_2 with varying packet sizes. Other parameters such as noise power spectral density ($N0$), Total transmitted power (P), Path loss exponent (n), distance (d), power channel gain (Ω) which is calculated as d^{-n}, channel use (m) and power allocation coefficients (β_1&β_2) are used to calculate the average BLER. The observed trend indicates that as the packet size increases, the total secrecy capacity also increases. This comes from the fact that the transmission rate increases as the packet size increases when all other parameters are fixed.

This unexpected increase in total secrecy capacity as packet size grows could stem from several underlying factors such as increased error correction capability and more efficient channel utilization.

Chapter 6

Conclusions and Future Work

6.1 Conclusions

The analysis of PLS for NOMA system setup described in chapter 3 has been a multifaceted journey into the intricacies of wireless communication reliability, security, and efficiency. Employing careful mathematical analyses and MATLAB generated visualizations, this study has unearthed pivotal insights into the performance of the NOMA systems under diverse scenarios. It has unraveled crucial insights into the interplay of parameters shaping the system's behavior.

Moreover, this study not only contributes to advancing the theoretical understanding of NOMA systems but also presents practical implications for real-world deployment. By explaining the impact of user proximity, transmitted signal power, path loss exponents, and packet sizes on system performance, it lays the groundwork for optimizing NOMA based wireless networks in practical settings. These findings provide a road-map for network engineers, policymakers, and researchers to develop robust and secure wireless communication infrastructures tailored to diverse application scenarios, spanning from IoT devices to mission critical communication systems.

The analysis of SINR distributions under varying channel conditions has illuminated the vulnerability of the NOMA system to fluctuations in wireless channel quality. This understanding serves as a foundation for devising adaptive strategies to counteract channel fluctuations and increase system performance. The dynamic nature of wireless channels poses challenges to maintaining consistent performance levels in communication systems. By recognizing the susceptibility of NOMA systems to channel variations, this study advocates for the implementation of dynamic resource allocation schemes and adaptive modulation techniques. Such strategies, capable of real-time adjustments based on channel quality feedback, can effectively mitigate the adverse effects of channel fluctuations. This adaptive approach not only ensures better utilization of resources but also increase s system resilience in the face of dynamic and unpredictable wireless environments, thereby bolstering the reliability and security of NOMA based wireless networks.

The BLER assessment unveiled the critical role of user proximity to the BS in influencing error rates and demonstrating a direct correlation between transmitted signal power and error reduction. This assessment underscores the criticality of optimizing these factors for minimizing transmission errors. The revelations about the influence of distance, channel conditions, and data block size on BLER provoke thoughtful considerations for system design and resource allocation.

In addition, the BLER analysis has highlighted the intricate relationship between system parameters and error probabilities within data blocks. It not only emphasizes the significance of optimizing user proximity and transmitted signal power but also underscores the dynamic nature of channel conditions and data block sizes in determining error rates. These findings compel a nuanced approach towards system design, necessitating adaptable strategies that account for varying distances, dynamic channel characteristics, and optimal data block sizes. Addressing these complexities becomes paramount for enabling robust, low-latency communications, especially in scenarios requiring high-reliability short packet transmissions. The analysis of secrecy capacity provided insights into the importance of transmitted signal strength in ensuring secure communication channels. It underscored the pivotal relationship between transmitted signal power and information confidentiality. The findings emphasized the significance of sufficient signal strength in ensuring secure communication channels, offering a road map into developing increased system optimization strategies for increased system performance.

The findings not only underscore the significance of signal strength but also highlight the delicate balance between data confidentiality and transmission efficiency. Understanding this balance is crucial, particularly in sectors such as healthcare, finance, and government, where data security is paramount. These insights open doors for tailored approaches in data encryption, transmission protocols, and network infrastructure design, ensuring a symbiotic relationship between secure communication channels and optimal data throughput. The insights gleaned from secrecy capacity analysis serve as a guiding beacon for industries navigating the complex landscape of wireless communication security and efficiency.

The unanticipated trends in BLER and secrecy capacity concerning varied path loss exponents challenge established assumptions. The analysis revealed trends in BLER and secrecy capacity concerning varying path loss exponents. This highlighted the intricate balance between signal attenuation, interference, and noise in determining system reliability, laying the groundwork for redefined optimization strategies.

The understanding of BLER and secrecy capacity concerning path loss exponent variations has direct implications for real-world system implementations. Optimizing NOMA systems for practical deployment, considering diverse environmental conditions and user distributions, becomes imperative. This study's revelations emphasize the need for adaptive and robust system designs capable of dynamically adjusting to changing channel conditions, user mobility, and evolving network landscapes. By recognizing and leveraging the intricate interplay of signal propagation characteristics, interference patterns, and noise profiles, future NOMA systems can be tailored to offer resilient and secure communication platforms, addressing the demands of increasingly dynamic and complex wireless environments.

The balance between data volume and error susceptibility based on packet size underscore the necessity of tailored packet design for minimizing transmission errors, thereby contributing to improved data reliability.

The findings regarding the impact of packet size on error susceptibility carry significant implications for real-world deployment of NOMA systems in various applications. In scenarios demanding URLC, such as industrial IoT, autonomous vehicles, or healthcare, understanding the trade-offs between data volume and error susceptibility becomes paramount. Tailoring packet designs to minimize transmission errors

not only increase s data reliability but also ensures the seamless and secure transmission of critical information. Moreover, these insights pave the way for optimized communication protocols in emerging technologies like 6G networks, where reliable short packet transmissions are fundamental. Implementing these findings in practical systems stands to revolutionize wireless communication paradigms, fostering a new era of secure and efficient data transmission across diverse sectors.

The findings of this study not only fulfill the set research objectives but also serve as a catalyst for advancing NOMA systems' performance. These insights are foundational, paving the way for continued advancements in secure and efficient wireless communication technologies.

The insights garnered from this study serve as a foundation for designing optimized strategies and protocols within NOMA frameworks, empowering future endeavors toward increased reliability, security, and efficiency in wireless communication technologies.

In essence, this study marks the initiation of a continuum, inviting further in-depth investigations and practical implementations. The implications derived from this research set the stage for the evolution of NOMA systems, advocating for their widespread adoption across diverse communication scenarios.

6.2 Limitations and Future Research Directions

The findings underscore the multifaceted nature of NOMA systems in the context of PLS for SPC. They not only contribute to a deeper understanding of system behavior but also pave the way for future research directions and practical implementations. Based on these insights, avenues for further research include

This study has done in the assumption that Rayleigh fading affects the channels between the BS and the users. Further investigations into diverse fading models beyond Rayleigh fading can elucidate their impact on system performance. This includes modeling scenarios involving Rician, Nakagami, or Weibull fading to comprehend real-world signal behavior.

This study has done in the assumption of single eavesdropper presence. Delving deeper into the implications of multiple or sophisticated eavesdropping scenarios on system security and reliability will enrich the understanding of NOMA's resilience against malicious interventions.

Bridging the gap between theoretical findings and practical applications by conducting in-depth evaluations of optimized NOMA systems in real-world scenarios will validate theoretical insights and facilitate seamless technology transfer.

Exploring adaptive resource allocation strategies based on real-time channel conditions and user dynamics can lead to the development of dynamic NOMA frameworks, enhancing system adaptability and efficiency.

While this study offers substantial insights into NOMA systems' performance within the realm of PLS for SPC, it's crucial to acknowledge its limitations. The investigation primarily focused on specific scenarios and parameters, potentially overlooking certain real-world complexities or variations. Future research endeavors could encompass broader contexts, considering multifaceted interference models, diverse user behaviors, and practical implementation challenges. Exploring the inter-

play between NOMA and emerging technologies, such as IoT or 6G communication paradigms, presents promising avenues for extending this study's applicability and relevance.

Moving beyond theoretical exploration, the translation of these research findings into practical implementations is imperative. Real-world deployment and validation of optimized NOMA systems in various operational environments, considering factors like hardware constraints, energy efficiency, and scalability, remain pivotal. Collaborations with industry stakeholders and integration of these insights into standardized protocols could expedite the adoption of NOMA systems, ushering in an era of increased wireless communication security and efficiency.

References

[1] R. Abozariba, M. K. Naeem, M. Patwary, M. Seyedebrahimi, P. Bull, and A. Aneiba, "Noma-based resource allocation and mobility enhancement framework for iot in next generation cellular networks," *IEEE Access*, vol. 7, pp. 29 158–29 172, 2019.

[2] S. Atapattu, N. Ross, Y. Jing, Y. He, and J. S. Evans, "Physical-layer security in full-duplex multi-hop multi-user wireless network with relay selection," *IEEE Transactions on Wireless Communications*, vol. 18, no. 2, pp. 1216–1232, 2019.

[3] R. Chen, C. Li, S. Yan, R. Malaney, and J. Yuan, "Physical layer security for ultra-reliable and low-latency communications," *IEEE Wireless Communications*, vol. 26, no. 5, pp. 6–11, 2019.

[4] T. M. C. Chu, H.-J. Zepernick, and T. Q. Duong, "On optimal channel uses in ultra-reliable short-packet relaying communications," in *2022 IEEE Ninth International Conference on Communications and Electronics (ICCE)*, 2022, pp. 13–17.

[5] L. Dai, B. Wang, Z. Ding, Z. Wang, S. Chen, and L. Hanzo, "A survey of non-orthogonal multiple access for 5g," *IEEE Communications Surveys Tutorials*, vol. 20, no. 3, pp. 2294–2323, 2018.

[6] C. Feng and H. Wang, "Secure short-packet communications at the physical layer for 5g and beyond," *IEEE Communications Standards Magazine*, vol. 5, no. 3, pp. 96–102, 2021.

[7] Y. Gu, H. Chen, Y. Li, and B. Vucetic, "Ultra-reliable short-packet communications: Half-duplex or full-duplex relaying?" *IEEE Wireless Communications Letters*, vol. 7, no. 3, pp. 348–351, 2018.

[8] A. Jehan and M. Zeeshan, "Comparative performance analysis of code-domain noma and power-domain noma," in *Proc. International Conference on Ubiquitous Information Management and Communication*, 2022, pp. 1–6.

[9] X. Sun, S. Yan, N. Yang, Z. Ding, C. Shen, and Z. Zhong, "Short-packet downlink transmission with non-orthogonal multiple access," *IEEE Transactions on Wireless Communications*, vol. 17, no. 7, pp. 4550–4564, 2018.

[10] G. N. Tran, S. Q. Nguyen, M. T. Nguyen, and S. Kim, "Optimal power allocation for non-orthogonal multiple access visible light communications with short packet and imperfect channel information," in *2022 International Conference on Advanced Technologies for Communications (ATC)*, 2022, pp. 234–238.

[11] T. H. Vu, T. V. Nguyen, T. T. Nguyen, V. N. Q. Bao, and S. Kim, "Short-packet communications in noma-cdrt iot networks with cochannel interference and imperfect sic," *IEEE Transactions on Vehicular Technology*, vol. 71, no. 5, pp. 5552–5557, 2022.

[12] Y. Yu, H. Chen, Y. Li, Z. Ding, and B. Vucetic, "On the performance of non-orthogonal multiple access in short-packet communications," *IEEE Communications Letters*, vol. 22, no. 3, pp. 590–593, 2018.

[13] J. Zhang, H. Chen, L. Gong, J. Cao, and Z. Gu, "The current research of iot security," in *2019 IEEE Fourth International Conference on Data Science in Cyberspace (DSC)*, 2019, pp. 346–353.

Appendix A

Supplemental Information

Faculty of Faculty, Blekinge Institute of Technology, 371 79 Karlskrona, Sweden